Inhibited Long Non-Coding RNA OIP5-AS1 Elevated microRNA-92a to Suppress Proliferation and Metastasis of Ovarian Cancer Cells by Silencing ITGA6

Yujue Wang
Sichuan Academy of Medical Science & Sichuan Provincial People's Hospital
Lingling Li
Sichuan Academy of Medical Science & Sichuan Provincial People's Hospital
Xun Zhang
Sichuan Academy of Medical Science and Sichuan Provincial People's Hospital
Xiaolan Zhao (Zhaoxiaonan2332@163.com)
Sichuan Academy of Medical Sciences and Sichuan People's Hospital

Research article

Keywords: Ovarian cancer, Long non-coding RNA opa-interacting protein 5 antisense transcript 1, MicroRNA-92a, Integrin alpha 6, Proliferation, Metastasis

Posted Date: October 9th, 2020

DOI: https://doi.org/10.21203/rs.3.rs-86230/v1

Version of Record: A version of this preprint was published at Journal of Ovarian Research on February 16th, 2022. See the published version at https://doi.org/10.1186/s13048-021-00937-3.

Abstract

Objective: Over the years, long non-coding RNAs (lncRNAs) and microRNAs (miRNAs) have been identified as essential biomarkers during the development of malignancies. This study was performed to verify the roles of lncRNA opa-interacting protein 5 antisense transcript 1 (OIP5-AS1) and miR-92a in ovarian cancer (OC).

Methods: OIP5-AS1, miR-92a and ITGA6 expression in tissues and cells was assessed. The screened OC cells were respectively with integrin alpha 6 (ITGA6)/OIP5-AS1 silenced vector, miR-92a mimic/inhibitor or their negative controls. The viability, migration, invasion and apoptosis of the cells were determined and the levels of epithelial-mesenchymal transition (EMT)-related proteins were also measured. The interactions between OIP5-AS1 and miR-92a, and between miR-92a and ITGA6 were confirmed by dual luciferase report gene assay and/or RNA pull-down assay.

Results: OIP5-AS1 and ITGA6 were upregulated while miR-92a was downregulated in OC tissues versus the adjacent normal tissues. Inhibited OIP5-AS1 or elevated miR-92a repressed EMT, viability, migration and invasion of OC cells, and promoted OC cell apoptosis. These effects that induced by silenced OIP5-AS1 could be reversed by miR-92a inhibitor. The reduction of ITGA6 restricted EMT in OC cells. MiR-92a was a target of OIP5-AS1 and ITGA6 was targeted by miR-92a.

Conclusion: OIP5-AS1 silencing promoted miR-92a to repress proliferation and metastasis of OC cells through inhibiting ITGA6. This research may provide potential biomarkers for OC.

Introduction

Ovarian cancer (OC) is the most fatal among all reproductive cancers, the 11st commonest type and the 5th major reason of cancer-related death in women [1]. It was estimated by the most recent global statistic that there were 295,414 newly diagnosed cases of OC each year and 184,799 OC-related annual death [2]. This high mortality rate is induced by the absent or nonspecific symptoms in early stages of OC, resulting in delayed diagnoses until late stages. More than 75% of OC cases were not diagnosed before advanced stages and the 5-year survival rate of late stage OC is about 30% [3]. In general, the initial treatments for OC are surgery and chemotherapy, which are effective for most patients. However, the recurrence appeared in around 80% of OC patients within several years and treatment for recurrence is seldom curative [4]. Thus, novel targets for OC treatment are urgently needed.

Long noncoding RNAs (lncRNA) are functional RNA molecules containing over 200 nucleotides. LncRNAs modulate the expression of key genes via epigenetic modification and transcriptional and post-transcriptional regulation [5]. It has been identified that lncRNA HOTTIP acted as a predictive role in OC prognosis [6] and lncRNA LINC00152 has been demonstrated to promote OC cell proliferation through regulating mitochondrial apoptosis pathways [7]. OPA-interacting protein 5 antisense transcript 1 (OIP5-AS1) situated at chromosome 15q15.1 and is evolutionarily conserved in vertebrates [8]. OIP5-AS1 has been revealed to participate in the progression of cervical cancer [9] and breast cancer [10]. Nevertheless,

the role of OIP5-AS1 in OC remains rarely studied. It is known that lncRNAs are able to repress miRNA functions via serving as competing endogenous RNAs (ceRNAs) in human diseases [11]. MicroRNAs (miRNAs) are non-coding RNAs comprised of about 22 nucleotides, which post-transcriptional function on gene expression [12]. Some particular miRNAs have been reported to be implicated in OC. For instance, miR-203a-3p regulated the biological behaviors of OC cells [13], and miR-1307 has been identified to affect the chemosensitivity of OC cells [14]. MiR-92a is one of the miRNAs that was considered to be related to the progression of OC [15] and aggressive breast cancer [16]. Nevertheless, the combined effect of OIP5-AS1 and miR-92a is still unexplored. Integrin alpha 6 (ITGA6) is a 150-kDa transmembrane protein [17] that has been revealed to be related to drug resistance and prognosis in OC [18]. However, the target relation between miR-92a and ITGA6 remains unexplored.

We designed this research to investigate the role of OIP5-AS1/miR-92a/ITGA6 axis in OC, and we speculate that OIP5-AS1 may serve as a ceRNA to sponge miR-92a, thus regulating the biological processes of OC cells with the involvement of ITGA6.

Materials And Methods

Ethics statement

Written informed consents were acquired from all patients before this study. The protocol of this study was confirmed by the Ethic Committee of Sichuan Academy of Medical Sciences Sichuan Provincial People's Hospital and based on the ethical principles for medical research involving human subjects of the Helsinki Declaration.

Study subjects

Paired OC tissues and adjacent normal tissues were harvested from 160 patients that accepted surgery in Sichuan Academy of Medical Sciences Sichuan Provincial People's Hospital between January 2017 and January 2019 and immediately preserved in liquid nitrogen for subsequent use. Age of the patients ranged from 18 to 80 years and the primary OC was confirmed pathologically by veteran pathologists. Additionally, patients with other malignant diseases or previous neoadjuvant chemotherapy or radiotherapy were excluded [19, 20].

Cell culture

Four OC cell lines (OVCAR3, SKOV3, A2780, and HO-8910) and human ovarian immortalized nontumorigenic ovarian surface epithelial cells (IOSE) were acquired from American Type Culture Collection (VA, USA) and cultured in Dulbecco’s modified Eagle medium (DMEM) (TransGen Biotech Co., Ltd., Beijing, China) containing 10% fetal bovine serum (Gibco Company, NY, USA) and 1% penicillin/streptomycin (Sigma-Aldrich Chemical Company., MO, USA). All the cells were incubated in humidified chambers [20].

Cell transfection

SKOV3 and A2780 cells were severally transfected with OIP5-AS1 silenced vector, miR-92a mimic/inhibitor, ITGA6 silenced vector or their respective negative control (NC) (Shanghai GenePharma Co., Ltd., Shanghai, China). The cells were cultured in 6-well plates until the cell confluence reached 70%-80%, and then transfected with plasmids by Lipofectamine 2000 (Invitrogen, CA, USA) according to the protocols.

Cell counting kit-8 (CCK-8) assay

The cell viability was determined in strict line with CCK-8 method (Dojindo Molecular Technologies Inc. Kumamoto, Japan). OC cells in each group were incubated on 96-well plates at 1000–3000 cells/well and the optical density was measured using a FLx800 Fluorescent Microplate Reader (BioTeke Corporation, Beijing, china).

Colony formation assay

The colony formation ability of cells was assessed in accordance with CytoSelect™ 96-well cell transformation assay (standard Soft Agar kits, Cell Biolabs Inc. CA, USA). Cells in each group were seeded onto 96-well plates at 5000 cells/well and incubated for 2 w. The clonies were detected by CyQuant and analyzed by a FLx800 fluorescent microplate reader (Biotek).

Transwell assay

Cells were suspended with 200 μL serum-free DMEM and seeded onto cell culture insert precoated with 1 μg/μL Matrigel. The basolateral chambers were appended with complete medium. Incubated for 48 h, the cells that did not penetrate through the membrane were removed, while the transmembrane cells were stained by 0.1% crystal violet dye solution. The numbers of migrated and invasive cells in five randomly fields were measured under a light microscope (Olympus Optical Co., Ltd, Tokyo, Japan).

Scratch test

OC cells were seeded and on the second day, cells covered the bottom of the plates. A 200 μL pipette tip was used to vertically scratched along the edge of a disinfected ruler (3 parallel scratches on each well). The supernatant was discarded and the wells were supplemented with serum-free medium to eliminate the effect induced by proliferation. Cells were photographed under a microscope after 24 h.

Flow cytometry

Transfected cells were collected after 48 -h transfection. Fluoresceine isothiocyanate Annexin V Apoptosis Detection Kits (BD Biosciences, Franklin Lakes, NJ, USA) were utilized to assess the apoptosis under a FACScan Flow Cytometer. The apoptosis rate was calculated by Cell Quest software (BD Biosciences).

Reverse transcription quantitative polymerase chain reaction (RT-qPCR)

Total RNA in tissues and cells was extracted by TRIzol kits (Invitrogen). A NanoDrop ND-3000 spectrophotometer (Thermo Fisher Scientific Inc., MA, USA) was employed for RNA quantification and the RNA was reversely transcribed into cDNA by PrimeScript RT Master Mix (TaKaRa Biotechnology Co., Ltd., Liaoning, China). The expression levels of target genes were affirmed by SYBR Premix Ex Taq II kits (TaKaRa) and the StepOnePlus system (Applied Biosystems Inc., CA, USA). Glyceraldehyde phosphate dehydrogenase (GAPDH) was used as the standardized control of OIP5-AS1 and ITGA6, and U6 was used as the standardized control of miR-92a. Data were analyzed using $2^{-\Delta\Delta Ct}$ method and the primer sequences were shown in Table 1.

Table 1
Primer sequence

Gene	Primer sequence (5'-3')
OIP5-AS1	F: 5'-TGCGAAGATGGCGGAGTAAG-3'
	R: 5'-TAGTTCCTCTCCTCTGGGGCCG-3'
miR-92a	F: 5'-ACACTCCAGCTGGGAGGTTGGGATTTGTCGC-3'
	R: 5'-CTCAACTGGTGTCGTGGAGTCGGCAATTCAGTTGAGA-3'
ITGA6	F: 5'-CACATCTCCTCCCTGAGCAC-3'
	R: 5'-TATCTTGCCACCCATCCTTG-3'
U6	F: 5'-GCTTCGGCAGCACATATACTAAAAT-3'
	R: 5'-CGCTTCACGAATTTGCGTGTCAT-3'
GAPDH	F: 5'-AAGGTGAAGGTCGGAGTCAA- 3'
	R: 5'-AATGAAGGGGTCATTGATGG-3'

Note: F, forward; R, reverse; OIP5-AS1, opa-interacting protein 5 antisense transcript 1; miR-92a, microRNA-92a; ITGA6, integrin alpha 6; GAPDH, glyceraldehyde phosphate dehydrogenase.

Western blot analysis

The proteins were extracted using radio-immunoprecipitation assay lysis buffer (Beyotime Biotechnology Co., Ltd., Shanghai, China). Equivalent proteins (20 μg) were separated on sodium dodecyl sulfate-polyacrylamide gel electrophoresis gel and transferred onto membranes for incubation with primary antibodies: ITGA6 (1: 10,000, Sigma), E-cadherin, vimentin (both 1: 1,000, Cell Signaling Technology, MA, USA) and GAPDH (1: 1,000, Santa Cruz Biotechnology Inc., CA, USA). Subsequently, the cells were incubated with horseradish peroxidase-conjugated secondary antibody and the bands were developed by Pierce™ enhanced chemiluminescent Western Blotting Substrate (32,109, Thermo Fisher). The signal intensities of proteins were evaluated using Image J software (Promega, WI, USA).

Dual luciferase reporter gene assay

Binding sites of OIP5-AS1 and miR-92a, miR-92a and ITGA6 were predicated by https://cm.jefferson.edu/ra22/Precomputed/ and http://www.targetscan.org/vert_72/. OIP5-AS1 and binding sequence of miR-92a containing its mutant sites were amplified by PCR and the PCR products were connected to pMirReporter plasmid (Sigma) to obtain OIP5-AS1 wild type (WT) vector (wt-OIP5-AS1) and OIP5-AS1 mutant type (MUT) vector (mut-OIP5-AS1). Similarly, ITGA6 WT (wt-ITGA6) and MUT (mut-ITGA6) report vectors were synthetized. Afterwards, Lipofectamine 3000 reagent (Thermo Fisher) was utilized to transfect WT/MUT vectors and miR-92a mimic or mimic-NC into SKOV3 and A2780 cells on 96-well plates for 24 h. The luciferase activity was determined.

RNA pull-down assay

The DNA fragment with OIP5-AS1 or its NC sequence was performed with PCR amplification through the T7-containing primer and bound to GV394 (Invitrogen). Plasmid DNA was digested with restriction enzyme XhoI and the biotin-labeled RNAs were reversely transcripted. Expression of target RNAs was determined by RT-qPCR based on the method in a former publication [21].

Statistical analysis

All data analyses were conducted using SPSS 21.0 software (IBM Corp. Armonk, NY, USA). The measurement data conforming to the normal distribution were expressed as mean ± standard deviation. The unpaired t-test was performed for comparisons between two groups, one-way analysis of variance (ANOVA) was used for comparisons among multiple groups and Tukey's post hoc test was used for pairwise comparisons after one-way ANOVA. P value < 0.05 was indicative of statistically significant difference.

Results

lncRNA OIP5-AS1 and ITGA6 are upregulated while miR-92a is downregulated in OC tissues

OIP5-AS1, miR-92a and ITGA6 expression in tissues were gauged and we found significant higher expression of OIP5-AS1 and ITGA6, and lower expression of miR-92a in OC tissues versus adjacent normal tissues (Fig. 1A, B).

Relationship between OIP5-AS1 expression and clinicopathological characteristics of OC patients

To further explore the relation between OIP5-AS1 expression and clinicopathological characteristics of OC patients, we divided the OC tissues in to the high expression group (n = 53) and the low expression group (n = 53) according to the median of OIP5-AS1 relative expression. The results suggested that OIP5-AS1 expression was higher in OC patients had advanced International Federation of Gynecology and Obstetrics (FIGO) stage (Fig. 1C), lymph node metastasis (LNM) (Fig. 1D) and larger tumor size (Fig. 1E).

Reduced OIP5-AS1 represses proliferation, migration, invasion and epithelial-mesenchymal transition (EMT) of OC cells, and accelerates cell apoptosis

SKOV3 and A2780 cells were selected for the determination of OC cell biological processes due to the high OIP5-AS1 expression in the two cell lines (Fig. 2A). In SKOV3 and A2780 cells, inhibition of OIP5-AS1 repressed viability, invasion and migration abilities, and also promoted apoptosis of OC cells. EMT-related protein expression were also influenced. Detailedly, the protein expression of E-cadherin was increased while that of vimentin was decreased by reduced OIP5-AS1 (Fig. 2B-G).

Elevated miR-92a constrains proliferation, migration, invasion and EMT of OC cells, and accelerates cell apoptosis

SKOV3 and A2780 cells had a lower expression level of miR-92a (Fig. 3A), so the two cell lines were selected for subsequent experiments. In SKOV3 and A2780 cells, the upregulation of miR-92a restrained viability, invasion and migration abilities, and also facilitated apoptosis of OC cells. Moreover, the protein expression of E-cadherin was heightened while that of vimentin was lowered after the treatment of miR-92a mimic (Fig. 3B-G).

Inhibition of miR-92a reverses the effects of degraded OIP5-AS1 on biological processes of OC cells

In SKOV3 and A2780 cells, reduced miR-92a was able to reverse the impacts of OIP5-AS1 silencing on viability, migration, invasion and apoptosis of OC cells; in relation to the sh-OIP5-AS1 group, the protein expression of E-cadherin was suppressed while that of vimentin was promoted in the sh-OIP5-AS1 + miR-92a inhibitor group (Fig. 4A-F).

MiR-92a is a target of OIP5-AS1

Target relation between miR-92a and OIP5-AS1 was evaluated by a bioinformatic website. It was further confirmed that miR-92a broadly inhibited the luciferase activity of wt-OIP5-AS1 and miR-929a inhibitor obviously strengthened the luciferase activity of wt-OIP5-AS1, while the effect was not found in mut-OIP5-AS1 (Fig. 5A), indicating a direct interaction between miR-92a and OIP5-AS1. Subsequently, RNA pull-down assay was used to confirm whether OIP5-AS1 could pull miR-92a down. We discovered that miR-92a was enriched in OC cells that had been pulled down by biotinylated OIP5-AS1 (Fig. 5B). Moreover, we found through RT-qPCR that OIP5-AS1 expression was lower while miR-92a expression was higher in the sh-OIP5-AS1 group versus the sh-NC group; OIP5-AS1 expression showed no difference while miR-92a was upregulated in the miR-92a mimic group when compared with the mimic-NC group; in contrast to the sh-OIP5-AS1 group, OIP5-AS1 expression didn't alter while miR-92a was downregulated in the sh-OIP5-AS1 + miR-92a inhibitor (Fig. 5C). These data showed that miR-92a directly bound to OIP5-AS1 at miRNA recognition site.

ITGA6 is targeted by miR-92a and the reduction of ITGA6 inhibits EMT of OC cells

A bioinformatic website was applied to predict the target relation between miR-92a and ITGA6. It was found in dual luciferase report gene assay that the overexpression of miR-92a apparently repressed activity of ITGA6 3'-untranslated region (3'UTR), while didn't affect the activity of mutant ITGA6 3'UTR; miR-92a inhibitor evidently promoted the activity of ITGA6 3'UTR, while didn't influence the activity of mutant ITGA6 3'UTR (Fig. 6A). Furthermore, we found that the sh-OIP5-AS1 and miR-92a mimic groups had lower expression of ITGA6 than the sh-NC group and the mimic-NC groups, respectively; in comparison to the sh-OIP5-AS1 group, ITGA6 was overexpressed in the sh-OIP5-AS1 + miR-92a inhibitor group (Fig. 6B, C).

It was observed in SKOV3 and A2780 cells that ITGA6 was knocked down after the treatment of si-ITGA6 (Fig. 6D). The expression levels of EMT-related proteins were measured and the outcomes suggested that the protein expression of E-cadherin was increased while that of vimentin was decreased in the si-ITGA6 group versus the si-NC group (Fig. 6E).

Discussion

OC is a malignancy that threatens women's health globally. Although the incidence of OC is lower than that of cervical and endometrial cancers, its mortality is the highest among all gynecological cancers [22]. Accumulating evidence has shown that lncRNAs are capable of acting as ceRNAs to sponge miRNAs, thus modulating cell functions [23]. This research was performed to explore the role of lncRNA OIP5-AS1 in the progression of OC by sponging miR-92a via regulating ITGA6, and the results of our experiments indicated that the reduction of OIP5-AS1 elevated miR-92a to repress proliferation and metastasis of OC cells through downregulating ITGA6.

To begin with, we determined the expression levels of OIP5-AS1, miR-92a and ITGA6 in tissues. It was found that OIP5-AS1 and ITGA6 were upregulated while miR-92a was downregulated in OC tissues when compared with adjacent tissues. Consistently, Song *et al*. have unveiled that OIP5-AS1 was highly expressed in cervical cancer tissues [9]. A previous study has suggested that miR-92a was downregulated in breast cancer cells [16], and it has been identified that the expression of ITGA6 was increased in cisplatin-resistant SKOV3 and cisplatin-resistant A2780 cells, and also in drug-resistant tissues in comparison to the controls [18]. The relationship between OIP5-AS1 and clinicopathological characteristics of OC patients has been analyzed and we discovered that the high expression of OIP5-AS1 was associated with advanced FIGO stage, LNM and larger tumor size of OC patients. Similarly, Yang *et al*. have affirmed that highly expressed OIP5-AS1 was related to advanced FIGO stage, LNM and poor overall survival of cervical cancer patients [24]. Moreover, we have found that OIP5-AS1 served as a ceRNA to absorb miR-92a, and ITGA6 was targeted by miR-92a. The regulatory relation between OIP5-AS1 and miR-92a remains unexplored while ITGA5 has been unraveled to be a target gene of miR-92a. However, the target relation of miR-92a and ITGA6 has not been studied yet.

Altered OIP5-AS1, miR-92a and ITGA6 were transfected into the OC cells to observe their roles in the biological behaviors of OC cells. The results of gain- and loss-of-function assays mirrored that silenced OIP5-AS1 or elevated miR-92a restrained proliferation, migration and invasion of OC cells, and also promoted OC cell apoptosis. In accordance with our findings, Wang *et al*. have found that OIP5-AS1 promoted proliferation of lung cancer cells [25]. OIP5-AS1 has also been demonstrated to aggravate proliferation and migration of gastric cancer cells, and the cell apoptosis was induced by silenced OIP5-AS1 [26]. A recent publication has uncovered that miR-92a-3p suppressed cell growth in Wilms' tumor [27]. Gu *et al*. have also illuminated that miR-92a inhibited proliferation and induced apoptosis in acute myeloid leukemia [28]. Moreover, the expression of E-cadherin and vimentin was determined in our study, and we found that the knockdown of OIP5-AS1/ITGA6 or elevation of miR-92a heightened E-cadherin expression while lowered vimentin expression, indicating their repressive roles in EMT progression in OC. In line with these results, Wang *et al*. have pointed out that overexpressed OIP5-AS1 facilitated EMT of laryngeal squamous cell carcinoma cells [29], and reduced OIP5-AS1 has been verified to inhibit EMT progress in hepatoblastoma cells [30]. Furthermore, it has been recently discovered that miR-92b inhibited EMT in triple negative breast cancer cells [31] and nasopharyngeal cancer cells [32]. In addition, Zhang *et al*. have clarified that the oncogenic K-Ras upregulated ITGA6 to promote EMT [33].

To sum up, our study revealed that OIP5-AS1 elevated miR-92a to suppress proliferation and metastasis of OC cells by silencing ITGA6. This research may be helpful for exploring therapeutic strategies for OC. However, more efforts are required to investigate the detailed mechanisms.

Declarations

Funding

None

Ethics approval and consent to participate

Written informed consents were acquired from all patients before this study. The protocol of this study was confirmed by the Ethic Committee of Sichuan Academy of Medical Sciences Sichuan Provincial People's Hospital and based on the ethical principles for medical research involving human subjects of the Helsinki Declaration.

Conflict of interest

The authors declare that they have no conflicts of interest.

Consent for publication

Not applicable

Availability of data and material

Not applicable

Authors' contributions

Xun Zhang and Xiaolan Zhao contributed to study design; Yujue Wang contributed to manuscript editing; Lingling Li contributed to experimental studies; Lingling Li contributed to data analysis.

Acknowledgement

We would like to acknowledge the reviewers for their helpful comments on this pap.

References

1. Shafabakhsh, R. and Z. Asemi, *Quercetin: a natural compound for ovarian cancer treatment.* J Ovarian Res, 2019. **12**(1): p. 55.
2. Bray, F., J. Ferlay, I. Soerjomataram, R.L. Siegel, L.A. Torre, and A. Jemal, *Global cancer statistics 2018: GLOBOCAN estimates of incidence and mortality worldwide for 36 cancers in 185 countries.* CA Cancer J Clin, 2018. **68**(6): p. 394-424.
3. Emmings, E., S. Mullany, Z. Chang, C.N. Landen, Jr., S. Linder, and M. Bazzaro, *Targeting Mitochondria for Treatment of Chemoresistant Ovarian Cancer.* Int J Mol Sci, 2019. **20**(1).
4. Kargo, A.S., A. Coulter, P.T. Jensen, and K.D. Steffensen, *Proactive use of PROMs in ovarian cancer survivors: a systematic review.* J Ovarian Res, 2019. **12**(1): p. 63.
5. Wang, X., W. Liu, P. Wang, and S. Li, *RNA interference of long noncoding RNA HOTAIR suppresses autophagy and promotes apoptosis and sensitivity to cisplatin in oral squamous cell carcinoma.* J Oral Pathol Med, 2018. **47**(10): p. 930-937.
6. Zou, T., P.L. Wang, Y. Gao, and W.T. Liang, *Long noncoding RNA HOTTIP is a significant indicator of ovarian cancer prognosis and enhances cell proliferation and invasion.* Cancer Biomark, 2019. **25**(2): p. 133-139.
7. Chen, P., X. Fang, B. Xia, Y. Zhao, Q. Li, and X. Wu, *Long noncoding RNA LINC00152 promotes cell proliferation through competitively binding endogenous miR-125b with MCL-1 by regulating mitochondrial apoptosis pathways in ovarian cancer.* Cancer Med, 2018. **7**(9): p. 4530-4541.
8. Sun, W.L., T. Kang, Y.Y. Wang, J.P. Sun, C. Li, H.J. Liu, Y. Yang, and B.H. Jiao, *Long noncoding RNA OIP5-AS1 targets Wnt-7b to affect glioma progression via modulation of miR-410.* Biosci Rep, 2019. **39**(1).
9. Song, L., L. Wang, X. Pan, and C. Yang, *lncRNA OIP5-AS1 targets ROCK1 to promote cell proliferation and inhibit cell apoptosis through a mechanism involving miR-143-3p in cervical cancer.* Braz J Med Biol Res, 2020. **53**(1): p. e8883.
10. Zeng, H., J. Wang, T. Chen, K. Zhang, J. Chen, L. Wang, H. Li, D. Tuluhong, J. Li, and S. Wang, *Downregulation of long non-coding RNA Opa interacting protein 5-antisense RNA 1 inhibits breast*

cancer progression by targeting sex-determining region Y-box 2 by microRNA-129-5p upregulation. Cancer Sci, 2019. **110**(1): p. 289-302.

11. Xu, J., J. Zhang, F. Shan, J. Wen, and Y. Wang, *SSTR5AS1 functions as a ceRNA to regulate CA2 by sponging miR15b5p for the development and prognosis of HBVrelated hepatocellular carcinoma.* Mol Med Rep, 2019. **20**(6): p. 5021-5031.
12. Jang, S.Y., M.K. Chae, J.H. Lee, E.J. Lee, and J.S. Yoon, *MicroRNA-27 inhibits adipogenic differentiation in orbital fibroblasts from patients with Graves' orbitopathy.* PLoS One, 2019. **14**(8): p. e0221077.
13. Liu, H.Y., Y.Y. Zhang, B.L. Zhu, F.Z. Feng, H.T. Zhang, H. Yan, and B. Zhou, *MiR-203a-3p regulates the biological behaviors of ovarian cancer cells through mediating the Akt/GSK-3beta/Snail signaling pathway by targeting ATM.* J Ovarian Res, 2019. **12**(1): p. 60.
14. Zhou, Y., M. Wang, T. Shuang, Y. Liu, Y. Zhang, and C. Shi, *MiR-1307 influences the chemotherapeutic sensitivity in ovarian cancer cells through the regulation of the CIC transcriptional repressor.* Pathol Res Pract, 2019. **215**(10): p. 152606.
15. Ohyagi-Hara, C., et al., *miR-92a inhibits peritoneal dissemination of ovarian cancer cells by inhibiting integrin alpha5 expression.* Am J Pathol, 2013. **182**(5): p. 1876-89.
16. Nilsson, S., C. Moller, K. Jirstrom, A. Lee, S. Busch, R. Lamb, and G. Landberg, *Downregulation of miR-92a is associated with aggressive breast cancer features and increased tumour macrophage infiltration.* PLoS One, 2012. **7**(4): p. e36051.
17. Zhang, D.H., Z.L. Yang, E.X. Zhou, X.Y. Miao, Q. Zou, J.H. Li, L.F. Liang, G.X. Zeng, and S.L. Chen, *Overexpression of Thy1 and ITGA6 is associated with invasion, metastasis and poor prognosis in human gallbladder carcinoma.* Oncol Lett, 2016. **12**(6): p. 5136-5144.
18. Wei, L., F. Yin, C. Chen, and L. Li, *Expression of integrin alpha-6 is associated with multi drug resistance and prognosis in ovarian cancer.* Oncol Lett, 2019. **17**(4): p. 3974-3980.
19. Li, X., S. Lin, Z. Mo, J. Jiang, H. Tang, C. Wu, and J. Song, *CircRNA_100395 inhibits cell proliferation and metastasis in ovarian cancer via regulating miR-1228/p53/epithelial-mesenchymal transition (EMT) axis.* J Cancer, 2020. **11**(3): p. 599-609.
20. Shi, Y., S. Gao, Y. Zheng, M. Yao, and F. Ruan, *LncRNA CASC15 Functions As An Unfavorable Predictor Of Ovarian Cancer Prognosis And Inhibits Tumor Progression Through Regulation Of miR-221/ARID1A Axis.* Onco Targets Ther, 2019. **12**: p. 8725-8736.
21. Wang, Y., Z. Liu, B. Yao, Q. Li, L. Wang, C. Wang, C. Dou, M. Xu, Q. Liu, and K. Tu, *Long non-coding RNA CASC2 suppresses epithelial-mesenchymal transition of hepatocellular carcinoma cells through CASC2/miR-367/FBXW7 axis.* Mol Cancer, 2017. **16**(1): p. 123.
22. Chen, S.N., R. Chang, L.T. Lin, C.U. Chern, H.W. Tsai, Z.H. Wen, Y.H. Li, C.J. Li, and K.H. Tsui, *MicroRNA in Ovarian Cancer: Biology, Pathogenesis, and Therapeutic Opportunities.* Int J Environ Res Public Health, 2019. **16**(9).
23. Li, M., Z. Xie, P. Wang, J. Li, W. Liu, S. Tang, Z. Liu, X. Wu, Y. Wu, and H. Shen, *The long noncoding RNA GAS5 negatively regulates the adipogenic differentiation of MSCs by modulating the miR-*

18a/CTGF axis as a ceRNA. Cell Death Dis, 2018. **9**(5): p. 554.

24. Yang, J., B. Jiang, J. Hai, S. Duan, X. Dong, and C. Chen, *Long noncoding RNA opa-interacting protein 5 antisense transcript 1 promotes proliferation and invasion through elevating integrin alpha6 expression by sponging miR-143-3p in cervical cancer.* J Cell Biochem, 2019. **120**(1): p. 907-916.
25. Wang, M., X. Sun, Y. Yang, and W. Jiao, *Long non-coding RNA OIP5-AS1 promotes proliferation of lung cancer cells and leads to poor prognosis by targeting miR-378a-3p.* Thorac Cancer, 2018. **9**(8): p. 939-949.
26. Bai, Y. and S. Li, *Long noncoding RNA OIP5-AS1 aggravates cell proliferation, migration in gastric cancer by epigenetically silencing NLRP6 expression via binding EZH2.* J Cell Biochem, 2020. **121**(1): p. 353-362.
27. Li, J.L. and P. Luo, *MiR-140-5p and miR-92a-3p suppress the cell proliferation, migration and invasion and promoted apoptosis in Wilms' tumor by targeting FRS2.* Eur Rev Med Pharmacol Sci, 2020. **24**(1): p. 97-108.
28. Gu, Y., J. Si, X. Xiao, Y. Tian, and S. Yang, *miR-92a Inhibits Proliferation and Induces Apoptosis by Regulating Methylenetetrahydrofolate Dehydrogenase 2 (MTHFD2) Expression in Acute Myeloid Leukemia.* Oncol Res, 2017. **25**(7): p. 1069-1079.
29. Wang, H., J. Qian, X. Xia, and B. Ye, *Long non-coding RNA OIP5-AS1 serves as an oncogene in laryngeal squamous cell carcinoma by regulating miR-204-5p/ZEB1 axis.* Naunyn Schmiedebergs Arch Pharmacol, 2020.
30. Zhang, Z., F. Liu, F. Yang, and Y. Liu, *Kockdown of OIP5-AS1 expression inhibits proliferation, metastasis and EMT progress in hepatoblastoma cells through up-regulating miR-186a-5p and down-regulating ZEB1.* Biomed Pharmacother, 2018. **101**: p. 14-23.
31. Li, Y.Y., X.H. Zheng, A.P. Deng, Y. Wang, J. Liu, Q. Zhou, G.Y. Cheng, and Q. Jiang, *MiR-92b inhibited cells EMT by targeting Gabra3 and predicted prognosis of triple negative breast cancer patients.* Eur Rev Med Pharmacol Sci, 2019. **23**(23): p. 10433-10442.
32. Zhao, C., F. Zhao, H. Feng, S. Xu, and G. Qin, *MicroRNA-92b inhibits epithelial-mesenchymal transition-induced migration and invasion by targeting Smad3 in nasopharyngeal cancer.* Oncotarget, 2017. **8**(53): p. 91603-91613.
33. Zhang, K., S.M. Myllymaki, P. Gao, R. Devarajan, V. Kytola, M. Nykter, G.H. Wei, and A. Manninen, *Oncogenic K-Ras upregulates ITGA6 expression via FOSL1 to induce anoikis resistance and synergizes with alphaV-Class integrins to promote EMT.* Oncogene, 2017. **36**(41): p. 5681-5694.

Figures

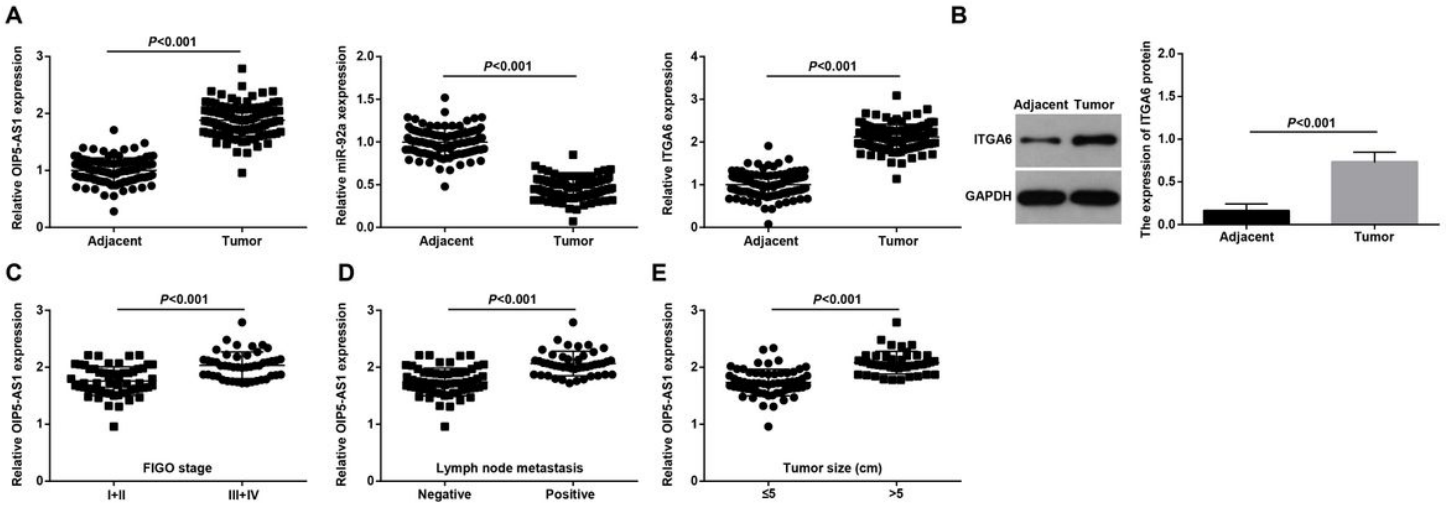

Figure 1

lncRNA OIP5-AS1 and ITGA6 are upregulated while miR-92a is downregulated in OC tissues; relationship between OIP5-AS1 expression and clinicopathological characteristics of OC patients. A, RT-qPCR was used to determine the expression of OIP5-AS1, miR-92a and ITGA6 in OC tissues; B, protein expression of ITGA6 in OC tissues was detected by Western blot analysis; C, relation between OIP5-AS1 expression and FIGO stage of OC patients; D, relation between OIP5-AS1 expression and LNM of OC patients; E, relation between OIP5-AS1 expression and tumor size of OC patients; A, B (n = 10), C, (I + II, n = 59; III + IV, n = 47), D, (positive, n = 45; negative, n = 61), E, (> 5, n = 45; ≤ 5, n = 61); the measurement data conforming to the normal distribution were expressed as mean ± standard deviation and the unpaired t-test was performed for comparisons between two groups.

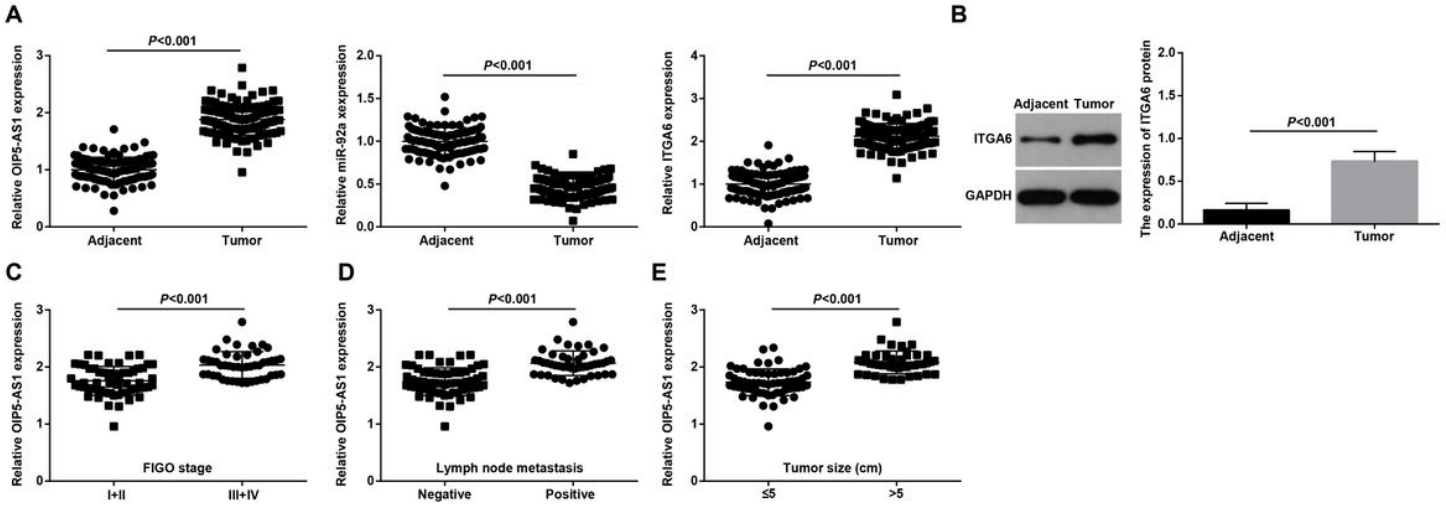

Figure 1

lncRNA OIP5-AS1 and ITGA6 are upregulated while miR-92a is downregulated in OC tissues; relationship between OIP5-AS1 expression and clinicopathological characteristics of OC patients. A, RT-qPCR was used to determine the expression of OIP5-AS1, miR-92a and ITGA6 in OC tissues; B, protein expression of

ITGA6 in OC tissues was detected by Western blot analysis; C, relation between OIP5-AS1 expression and FIGO stage of OC patients; D, relation between OIP5-AS1 expression and LNM of OC patients; E, relation between OIP5-AS1 expression and tumor size of OC patients; A, B (n = 10), C, (I + II, n = 59; III + IV, n = 47), D, (positive, n = 45; negative, n = 61), E, (> 5, n = 45; ≤ 5, n = 61); the measurement data conforming to the normal distribution were expressed as mean ± standard deviation and the unpaired t-test was performed for comparisons between two groups.

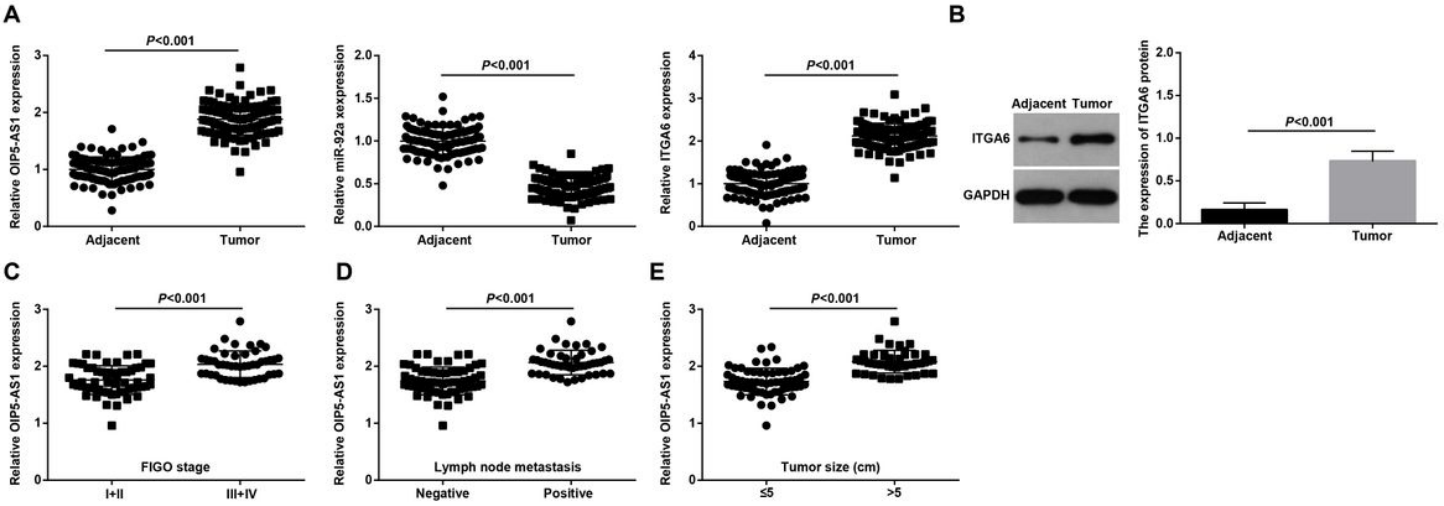

Figure 1

lncRNA OIP5-AS1 and ITGA6 are upregulated while miR-92a is downregulated in OC tissues; relationship between OIP5-AS1 expression and clinicopathological characteristics of OC patients. A, RT-qPCR was used to determine the expression of OIP5-AS1, miR-92a and ITGA6 in OC tissues; B, protein expression of ITGA6 in OC tissues was detected by Western blot analysis; C, relation between OIP5-AS1 expression and FIGO stage of OC patients; D, relation between OIP5-AS1 expression and LNM of OC patients; E, relation between OIP5-AS1 expression and tumor size of OC patients; A, B (n = 10), C, (I + II, n = 59; III + IV, n = 47), D, (positive, n = 45; negative, n = 61), E, (> 5, n = 45; ≤ 5, n = 61); the measurement data conforming to the normal distribution were expressed as mean ± standard deviation and the unpaired t-test was performed for comparisons between two groups.

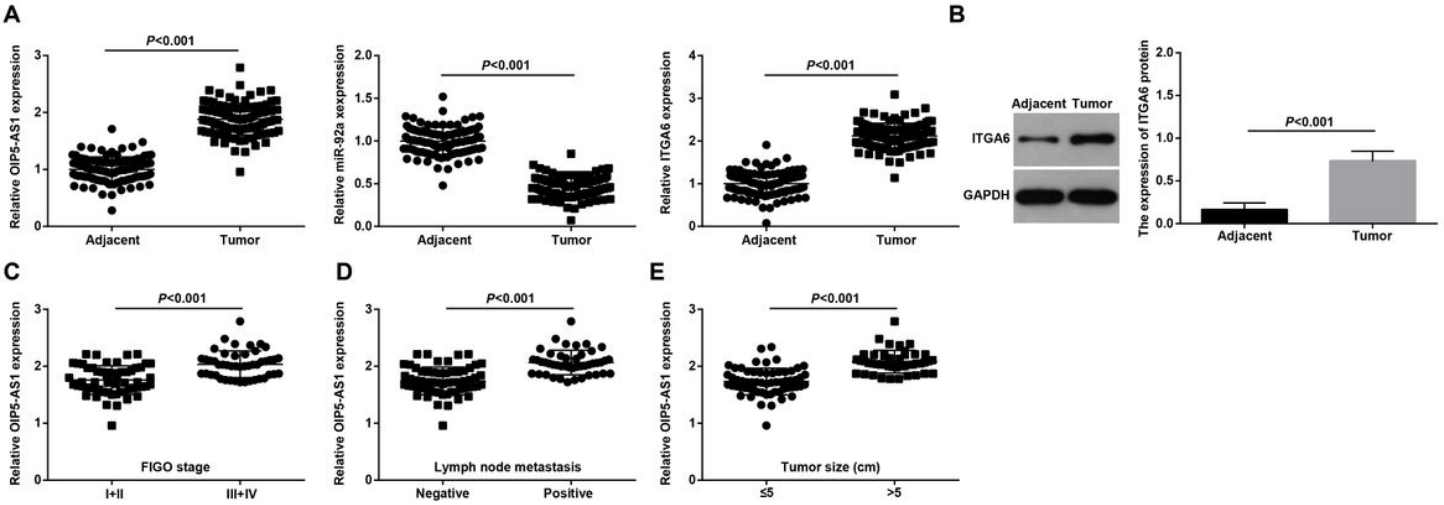

Figure 1

lncRNA OIP5-AS1 and ITGA6 are upregulated while miR-92a is downregulated in OC tissues; relationship between OIP5-AS1 expression and clinicopathological characteristics of OC patients. A, RT-qPCR was used to determine the expression of OIP5-AS1, miR-92a and ITGA6 in OC tissues; B, protein expression of ITGA6 in OC tissues was detected by Western blot analysis; C, relation between OIP5-AS1 expression and FIGO stage of OC patients; D, relation between OIP5-AS1 expression and LNM of OC patients; E, relation between OIP5-AS1 expression and tumor size of OC patients; A, B (n = 10), C, (I + II, n = 59; III + IV, n = 47), D, (positive, n = 45; negative, n = 61), E, (> 5, n = 45; ≤ 5, n = 61); the measurement data conforming to the normal distribution were expressed as mean ± standard deviation and the unpaired t-test was performed for comparisons between two groups.

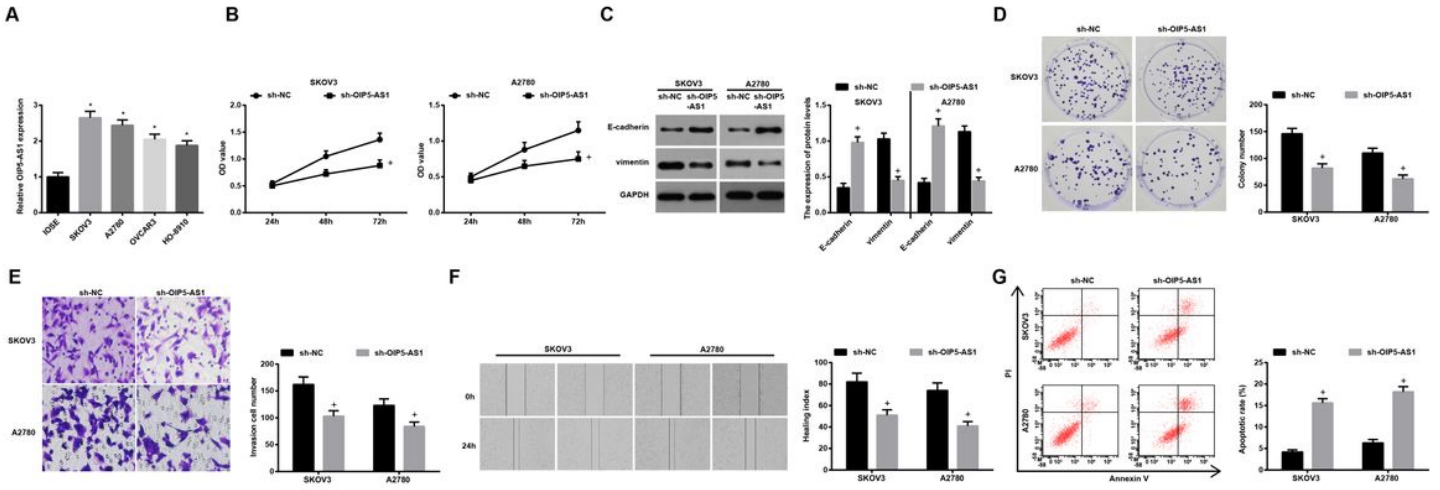

Figure 2

Reduced OIP5-AS1 represses proliferation, migration, invasion and EMT of OC cells, and accelerates cell apoptosis. A, OIP5-AS1 expression in OC cell lines was assessed using RT-qPCR; B, viability of SKOV3 and A2780 cells was detected by CCK-8 assay; C, expression of EMT-related proteins in OC cells was measured by Western blot analysis; D, colony formation ability of SKOV3 and A2780 cells was detected by colony formation assay; E, Transwell assay was employed to determine the invasion ability of SKOV3 and A2780 cells; F, migration ability of SKOV3 and A2780 cells was evaluated by scratch test; G, apoptosis rates of SKOV3 and A2780 cells were measured by flow cytometry; * P < 0.05 vs IOSE, + P < 0.05 vs the sh-NC group; N = 3, the measurement data conforming to the normal distribution were expressed as mean ± standard deviation, unpaired t-test was performed for comparisons between two groups, one-way ANOVA was used for comparisons among multiple groups and Tukey's post hoc test was used for pairwise comparisons after one-way ANOVA.

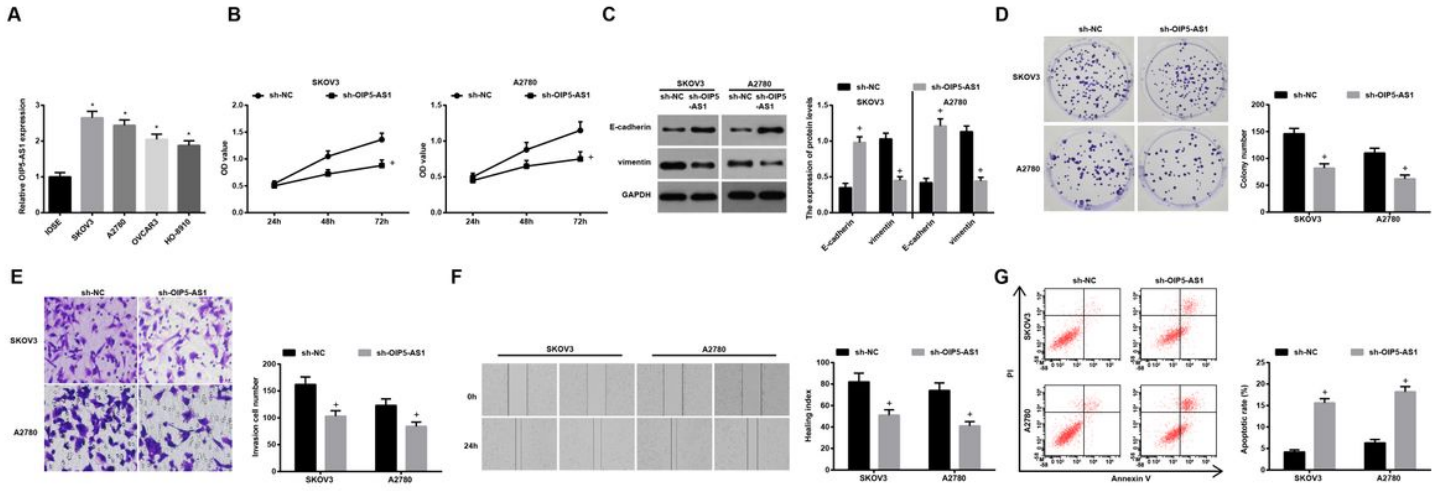

Figure 2

Reduced OIP5-AS1 represses proliferation, migration, invasion and EMT of OC cells, and accelerates cell apoptosis. A, OIP5-AS1 expression in OC cell lines was assessed using RT-qPCR; B, viability of SKOV3 and A2780 cells was detected by CCK-8 assay; C, expression of EMT-related proteins in OC cells was measured by Western blot analysis; D, colony formation ability of SKOV3 and A2780 cells was detected by colony formation assay; E, Transwell assay was employed to determine the invasion ability of SKOV3 and A2780 cells; F, migration ability of SKOV3 and A2780 cells was evaluated by scratch test; G, apoptosis rates of SKOV3 and A2780 cells were measured by flow cytometry; * $P < 0.05$ vs IOSE, + $P < 0.05$ vs the sh-NC group; N = 3, the measurement data conforming to the normal distribution were expressed as mean ± standard deviation, unpaired t-test was performed for comparisons between two groups, one-way ANOVA was used for comparisons among multiple groups and Tukey's post hoc test was used for pairwise comparisons after one-way ANOVA.

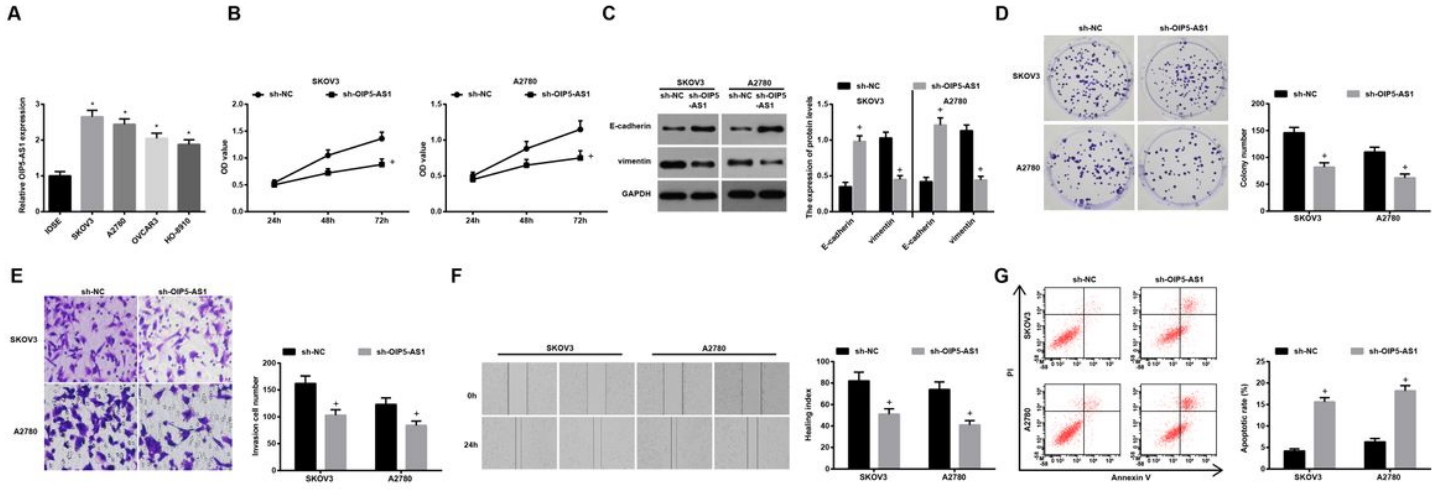

Figure 2

Reduced OIP5-AS1 represses proliferation, migration, invasion and EMT of OC cells, and accelerates cell apoptosis. A, OIP5-AS1 expression in OC cell lines was assessed using RT-qPCR; B, viability of SKOV3 and A2780 cells was detected by CCK-8 assay; C, expression of EMT-related proteins in OC cells was measured by Western blot analysis; D, colony formation ability of SKOV3 and A2780 cells was detected by colony formation assay; E, Transwell assay was employed to determine the invasion ability of SKOV3 and A2780 cells; F, migration ability of SKOV3 and A2780 cells was evaluated by scratch test; G, apoptosis rates of SKOV3 and A2780 cells were measured by flow cytometry; * P < 0.05 vs IOSE, + P < 0.05 vs the sh-NC group; N = 3, the measurement data conforming to the normal distribution were expressed as mean ± standard deviation, unpaired t-test was performed for comparisons between two groups, one-way ANOVA was used for comparisons among multiple groups and Tukey's post hoc test was used for pairwise comparisons after one-way ANOVA.

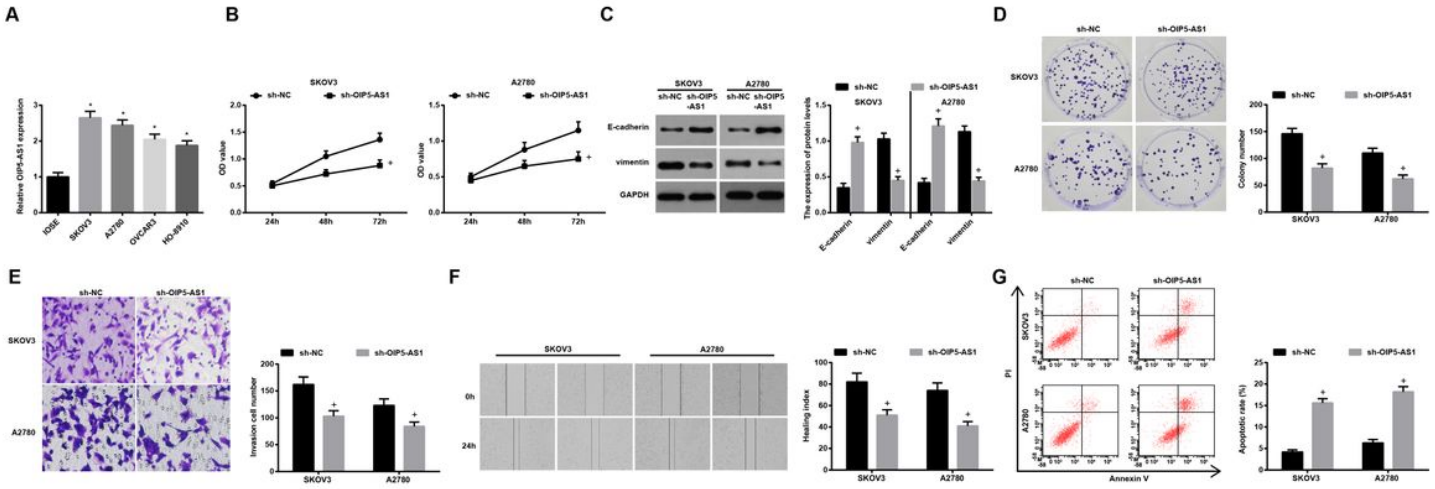

Figure 2

Reduced OIP5-AS1 represses proliferation, migration, invasion and EMT of OC cells, and accelerates cell apoptosis. A, OIP5-AS1 expression in OC cell lines was assessed using RT-qPCR; B, viability of SKOV3 and A2780 cells was detected by CCK-8 assay; C, expression of EMT-related proteins in OC cells was measured by Western blot analysis; D, colony formation ability of SKOV3 and A2780 cells was detected by colony formation assay; E, Transwell assay was employed to determine the invasion ability of SKOV3 and A2780 cells; F, migration ability of SKOV3 and A2780 cells was evaluated by scratch test; G, apoptosis rates of SKOV3 and A2780 cells were measured by flow cytometry; * P < 0.05 vs IOSE, + P < 0.05 vs the sh-NC group; N = 3, the measurement data conforming to the normal distribution were expressed as mean ± standard deviation, unpaired t-test was performed for comparisons between two groups, one-way ANOVA was used for comparisons among multiple groups and Tukey's post hoc test was used for pairwise comparisons after one-way ANOVA.

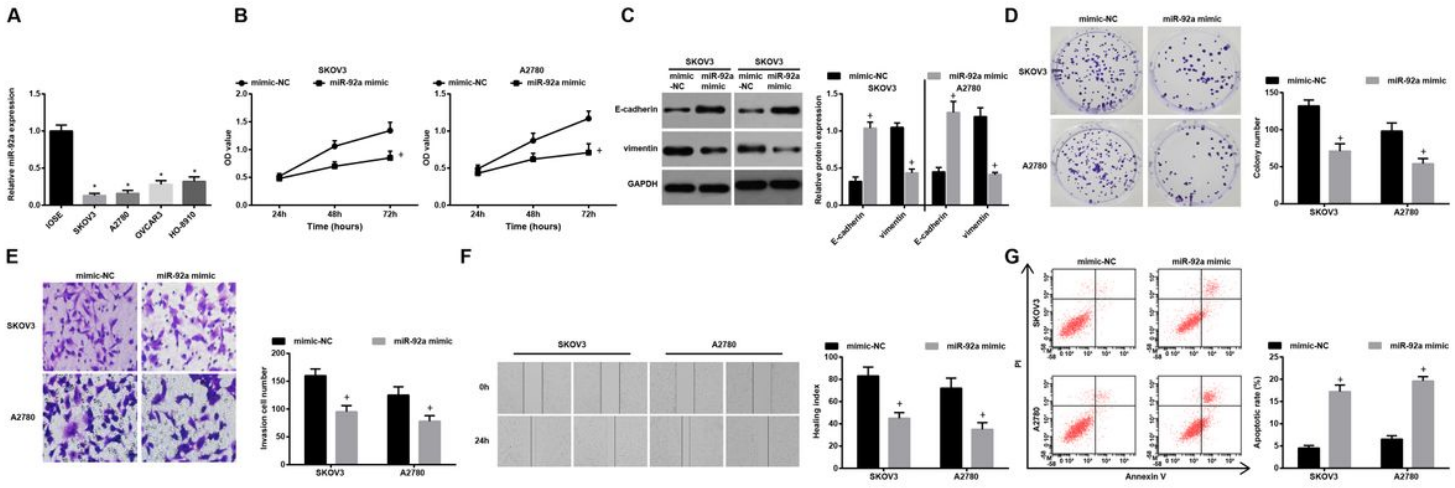

Figure 3

Elevated miR-92a constrains proliferation, migration, invasion and EMT of OC cells, and accelerates cell apoptosis. A, miR-92a expression in OC cell lines was assessed using RT-qPCR; B, viability of SKOV3 and A2780 cells was detected by CCK-8 assay; C, expression of EMT-related proteins in OC cells was measured by Western blot analysis; D, colony formation ability of SKOV3 and A2780 cells was detected by colony formation assay; E, Transwell assay was employed to determine the invasion ability of SKOV3 and A2780 cells; F, migration ability of SKOV3 and A2780 cells was evaluated by scratch test; G, apoptosis rates of SKOV3 and A2780 cells were measured by flow cytometry; * $P < 0.05$ vs IOSE, + $P < 0.05$ vs the mimic-NC group; N = 3, the measurement data conforming to the normal distribution were expressed as mean ± standard deviation, unpaired t-test was performed for comparisons between two groups, one-way ANOVA was used for comparisons among multiple groups and Tukey's post hoc test was used for pairwise comparisons after one-way ANOVA.

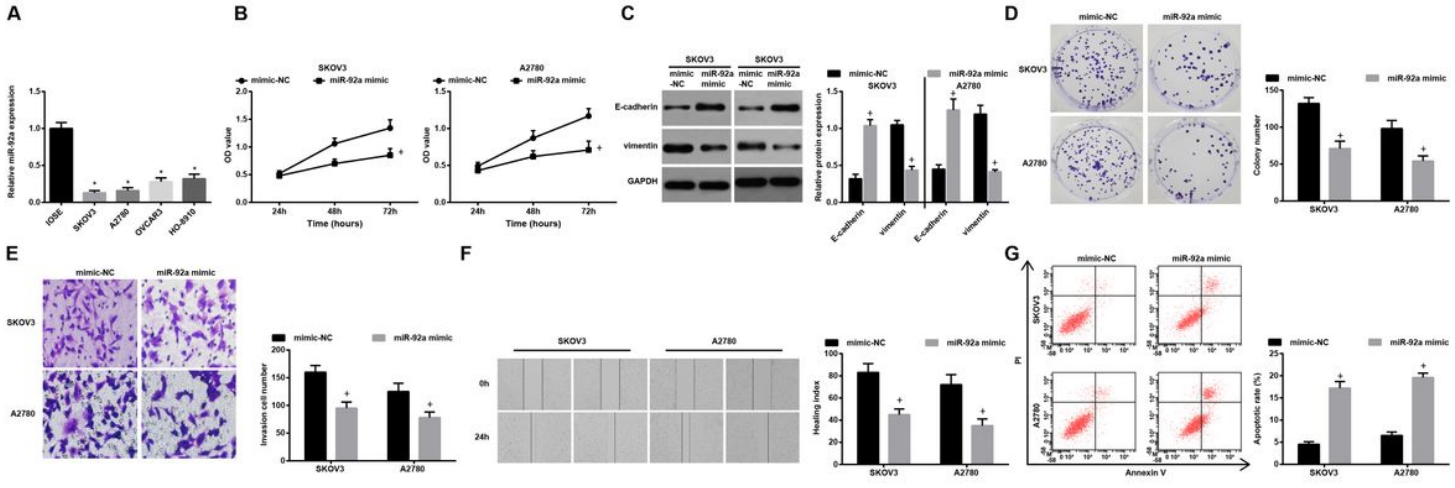

Figure 3

Elevated miR-92a constrains proliferation, migration, invasion and EMT of OC cells, and accelerates cell apoptosis. A, miR-92a expression in OC cell lines was assessed using RT-qPCR; B, viability of SKOV3 and

A2780 cells was detected by CCK-8 assay; C, expression of EMT-related proteins in OC cells was measured by Western blot analysis; D, colony formation ability of SKOV3 and A2780 cells was detected by colony formation assay; E, Transwell assay was employed to determine the invasion ability of SKOV3 and A2780 cells; F, migration ability of SKOV3 and A2780 cells was evaluated by scratch test; G, apoptosis rates of SKOV3 and A2780 cells were measured by flow cytometry; * P < 0.05 vs IOSE, + P < 0.05 vs the mimic-NC group; N = 3, the measurement data conforming to the normal distribution were expressed as mean ± standard deviation, unpaired t-test was performed for comparisons between two groups, one-way ANOVA was used for comparisons among multiple groups and Tukey's post hoc test was used for pairwise comparisons after one-way ANOVA.

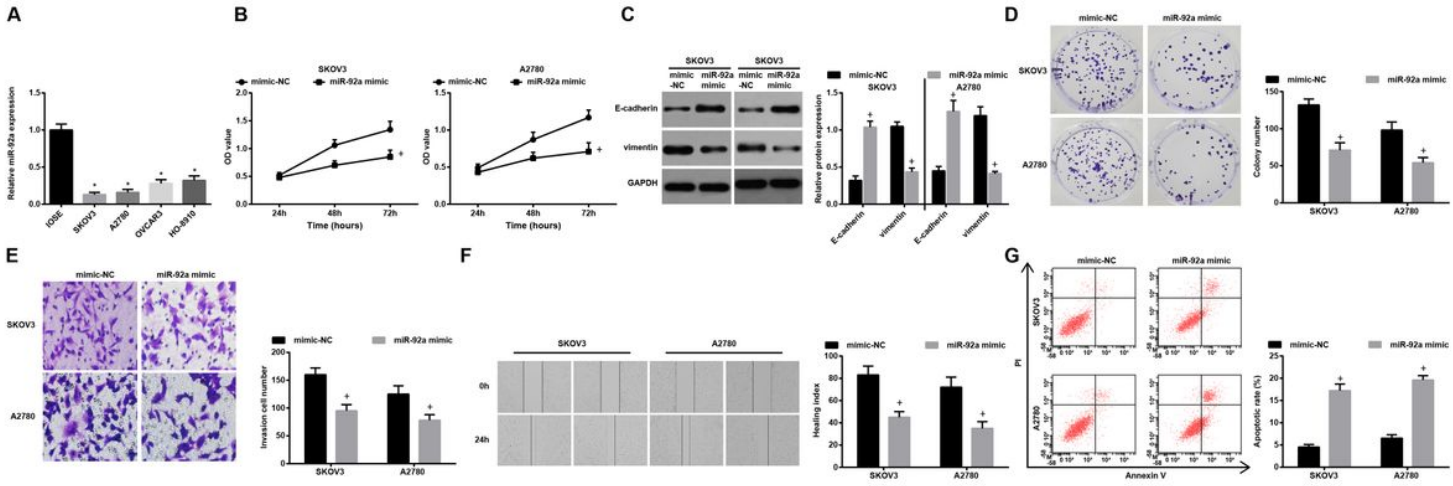

Figure 3

Elevated miR-92a constrains proliferation, migration, invasion and EMT of OC cells, and accelerates cell apoptosis. A, miR-92a expression in OC cell lines was assessed using RT-qPCR; B, viability of SKOV3 and A2780 cells was detected by CCK-8 assay; C, expression of EMT-related proteins in OC cells was measured by Western blot analysis; D, colony formation ability of SKOV3 and A2780 cells was detected by colony formation assay; E, Transwell assay was employed to determine the invasion ability of SKOV3 and A2780 cells; F, migration ability of SKOV3 and A2780 cells was evaluated by scratch test; G, apoptosis rates of SKOV3 and A2780 cells were measured by flow cytometry; * P < 0.05 vs IOSE, + P < 0.05 vs the mimic-NC group; N = 3, the measurement data conforming to the normal distribution were expressed as mean ± standard deviation, unpaired t-test was performed for comparisons between two groups, one-way ANOVA was used for comparisons among multiple groups and Tukey's post hoc test was used for pairwise comparisons after one-way ANOVA.

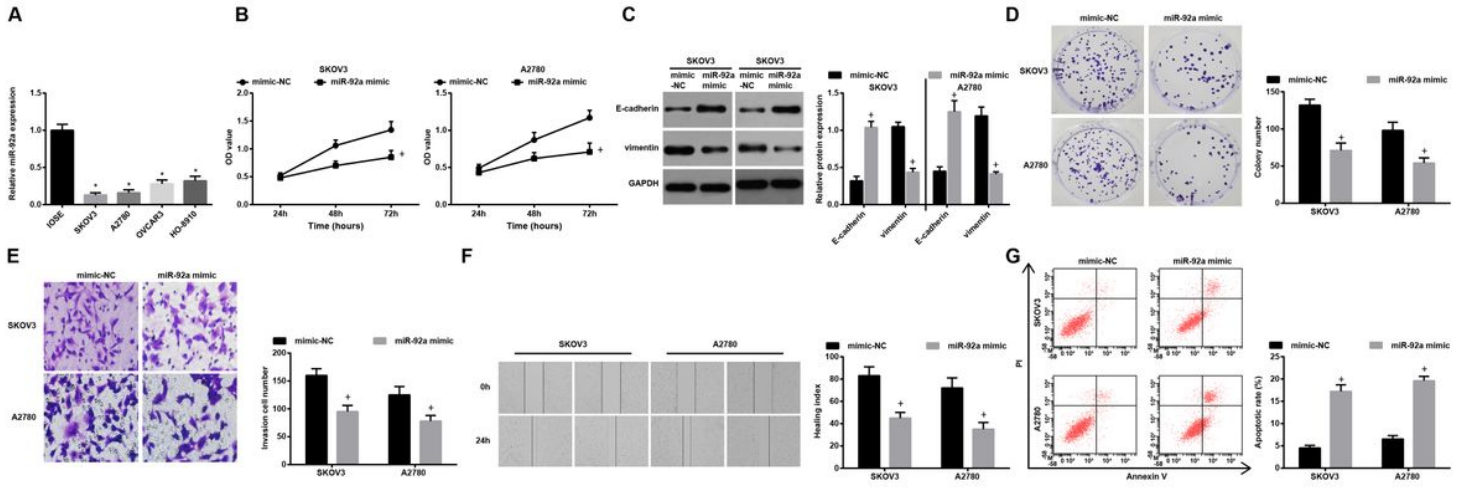

Figure 3

Elevated miR-92a constrains proliferation, migration, invasion and EMT of OC cells, and accelerates cell apoptosis. A, miR-92a expression in OC cell lines was assessed using RT-qPCR; B, viability of SKOV3 and A2780 cells was detected by CCK-8 assay; C, expression of EMT-related proteins in OC cells was measured by Western blot analysis; D, colony formation ability of SKOV3 and A2780 cells was detected by colony formation assay; E, Transwell assay was employed to determine the invasion ability of SKOV3 and A2780 cells; F, migration ability of SKOV3 and A2780 cells was evaluated by scratch test; G, apoptosis rates of SKOV3 and A2780 cells were measured by flow cytometry; * $P < 0.05$ vs IOSE, + $P < 0.05$ vs the mimic-NC group; N = 3, the measurement data conforming to the normal distribution were expressed as mean ± standard deviation, unpaired t-test was performed for comparisons between two groups, one-way ANOVA was used for comparisons among multiple groups and Tukey's post hoc test was used for pairwise comparisons after one-way ANOVA.

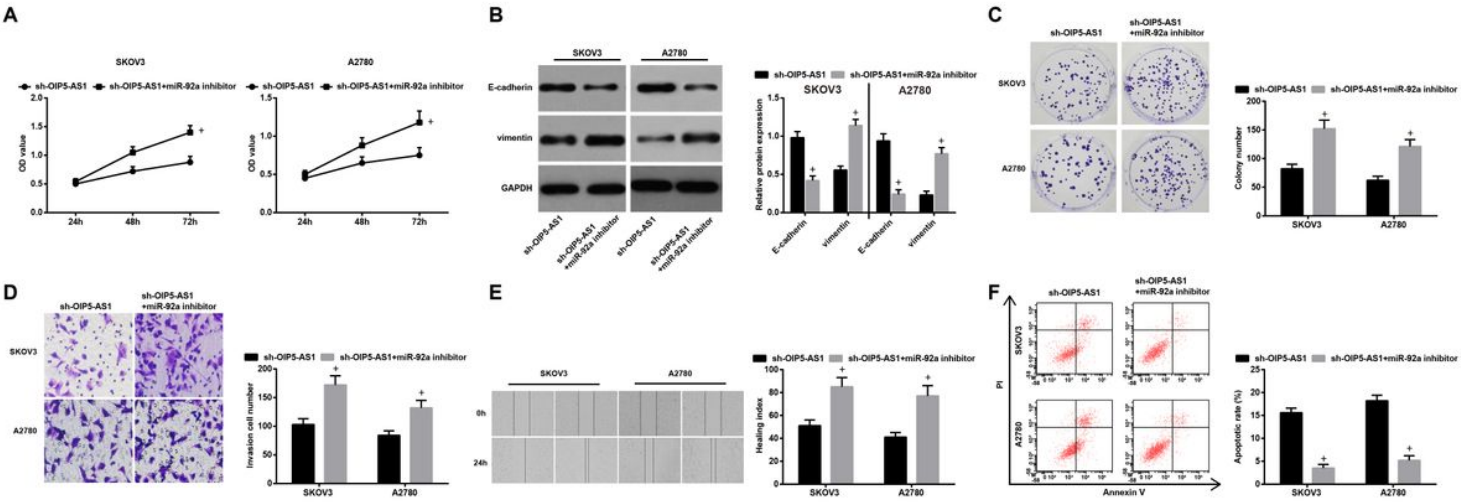

Figure 4

Inhibition of miR-92a reverses the effects of degraded OIP5-AS1 on biological processes of OC cells. A, viability of SKOV3 and A2780 cells was detected by CCK-8 assay; B, expression of EMT-related proteins in

OC cells was measured by Western blot analysis; C, colony formation ability of SKOV3 and A2780 cells was detected by colony formation assay; D, Transwell assay was employed to determine the invasion ability of SKOV3 and A2780 cells; E, migration ability of SKOV3 and A2780 cells was evaluated by scratch test; F, apoptosis rates of SKOV3 and A2780 cells were measured by flow cytometry; + P < 0.05 vs the sh-OIP5-AS1 group; N = 3, the measurement data conforming to the normal distribution were expressed as mean ± standard deviation and the unpaired t-test was performed for comparisons between two groups.

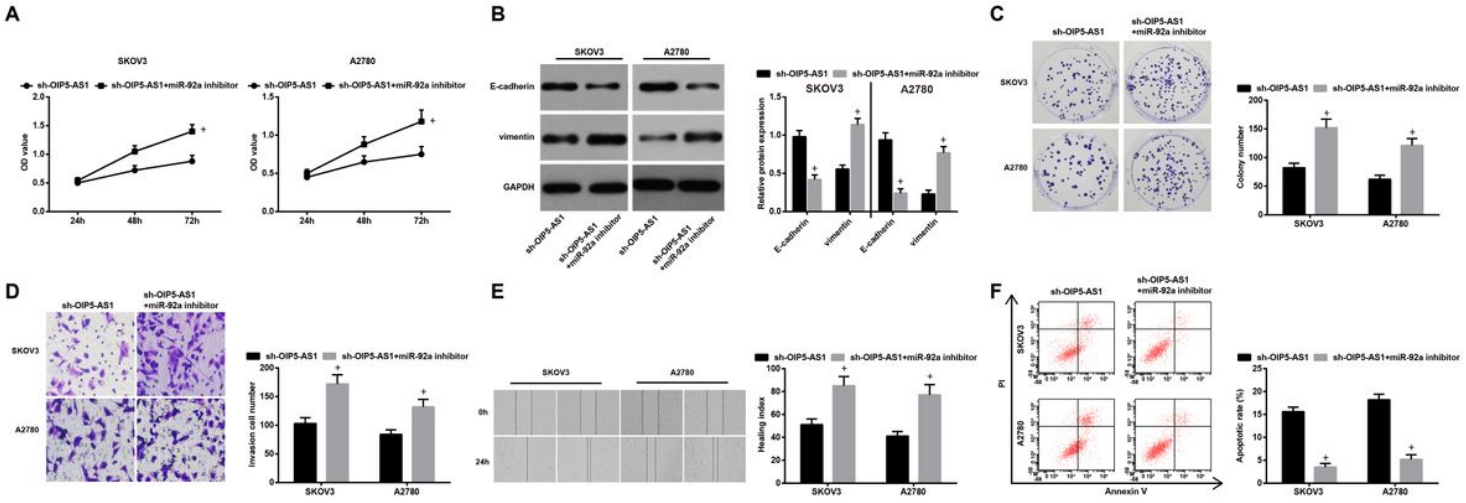

Figure 4

Inhibition of miR-92a reverses the effects of degraded OIP5-AS1 on biological processes of OC cells. A, viability of SKOV3 and A2780 cells was detected by CCK-8 assay; B, expression of EMT-related proteins in OC cells was measured by Western blot analysis; C, colony formation ability of SKOV3 and A2780 cells was detected by colony formation assay; D, Transwell assay was employed to determine the invasion ability of SKOV3 and A2780 cells; E, migration ability of SKOV3 and A2780 cells was evaluated by scratch test; F, apoptosis rates of SKOV3 and A2780 cells were measured by flow cytometry; + P < 0.05 vs the sh-OIP5-AS1 group; N = 3, the measurement data conforming to the normal distribution were expressed as mean ± standard deviation and the unpaired t-test was performed for comparisons between two groups.

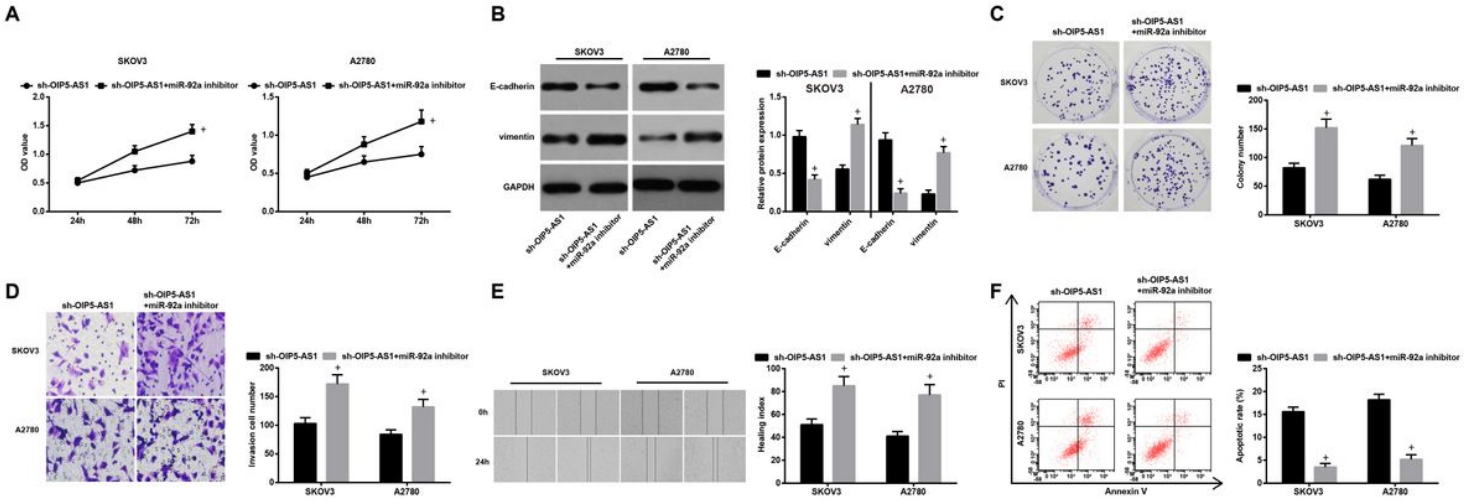

Figure 4

Inhibition of miR-92a reverses the effects of degraded OIP5-AS1 on biological processes of OC cells. A, viability of SKOV3 and A2780 cells was detected by CCK-8 assay; B, expression of EMT-related proteins in OC cells was measured by Western blot analysis; C, colony formation ability of SKOV3 and A2780 cells was detected by colony formation assay; D, Transwell assay was employed to determine the invasion ability of SKOV3 and A2780 cells; E, migration ability of SKOV3 and A2780 cells was evaluated by scratch test; F, apoptosis rates of SKOV3 and A2780 cells were measured by flow cytometry; + $P < 0.05$ vs the sh-OIP5-AS1 group; N = 3, the measurement data conforming to the normal distribution were expressed as mean ± standard deviation and the unpaired t-test was performed for comparisons between two groups.

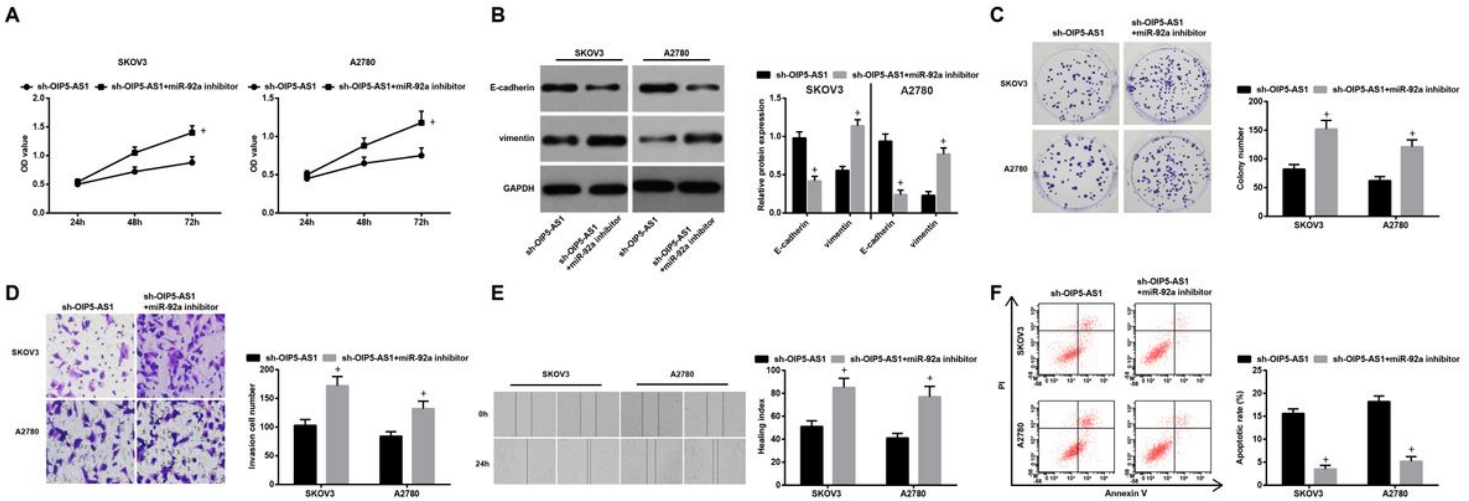

Figure 4

Inhibition of miR-92a reverses the effects of degraded OIP5-AS1 on biological processes of OC cells. A, viability of SKOV3 and A2780 cells was detected by CCK-8 assay; B, expression of EMT-related proteins in OC cells was measured by Western blot analysis; C, colony formation ability of SKOV3 and A2780 cells was detected by colony formation assay; D, Transwell assay was employed to determine the invasion

ability of SKOV3 and A2780 cells; E, migration ability of SKOV3 and A2780 cells was evaluated by scratch test; F, apoptosis rates of SKOV3 and A2780 cells were measured by flow cytometry; + P < 0.05 vs the sh-OIP5-AS1 group; N = 3, the measurement data conforming to the normal distribution were expressed as mean ± standard deviation and the unpaired t-test was performed for comparisons between two groups.

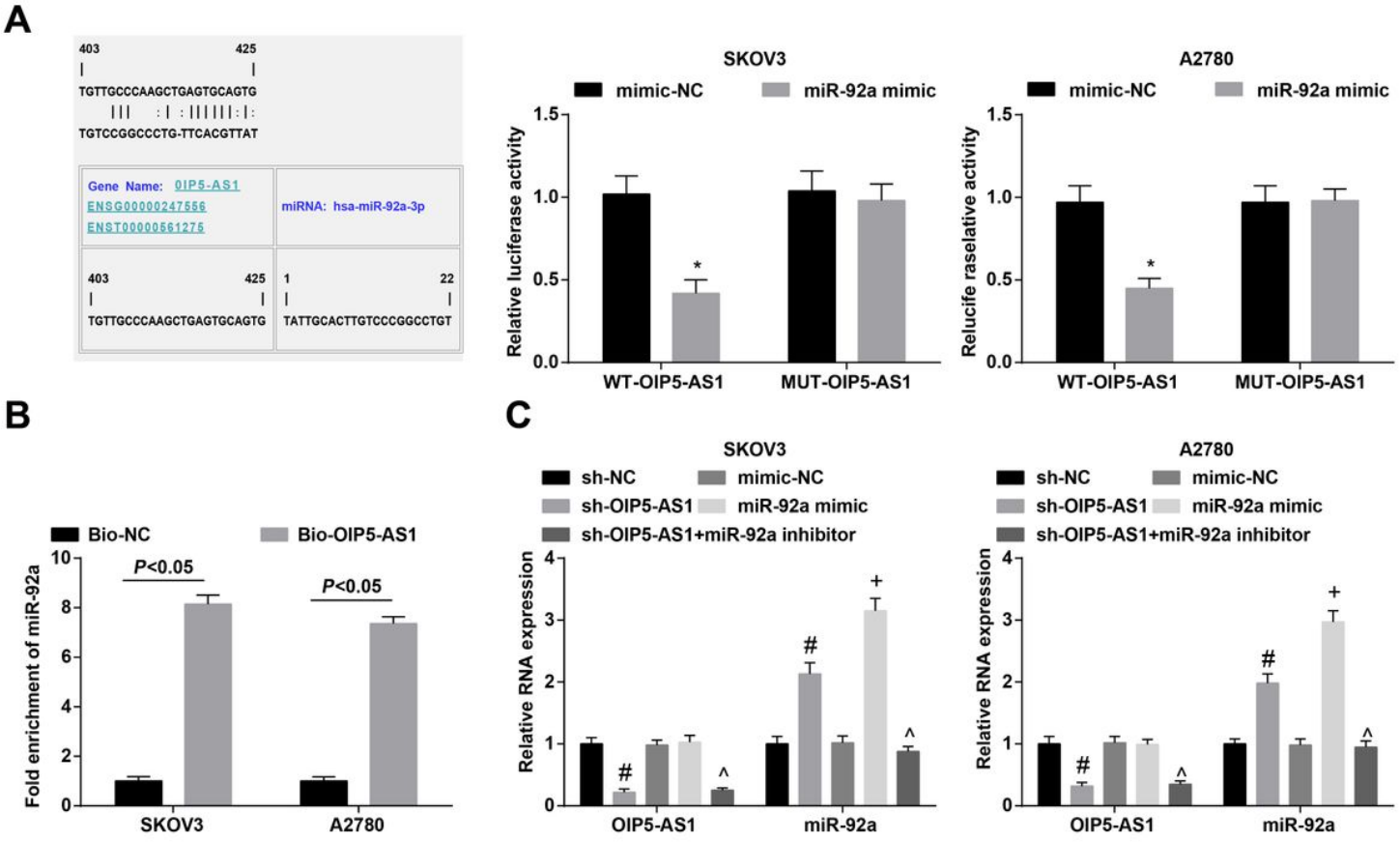

Figure 5

MiR-92a is a target of OIP5-AS1. A, binding sites of miR-92a and OIP5-AS1 were predicted by a bioinformatic website and the relationship between miR-92a and OIP5-AS1 was confirmed by dual luciferase report gene assay; B, RNA pull-down assay was used to affirm the regulatory relation between miR-92a and OIP5-AS1; C, expression of OIP5-AS1 and miR-92a in OC cells was determined by RT-qPCR; * P < 0.05 vs the anti-NC group, + P < 0.05 vs the mimic-NC group, # P < 0.05 vs the sh-NC group, ^ P < 0.05 vs the sh-OIP5-AS1 group; N = 3, the measurement data conforming to the normal distribution were expressed as mean ± standard deviation, unpaired t-test was performed for comparisons between two groups, one-way ANOVA was used for comparisons among multiple groups and Tukey's post hoc test was used for pairwise comparisons after one-way ANOVA.

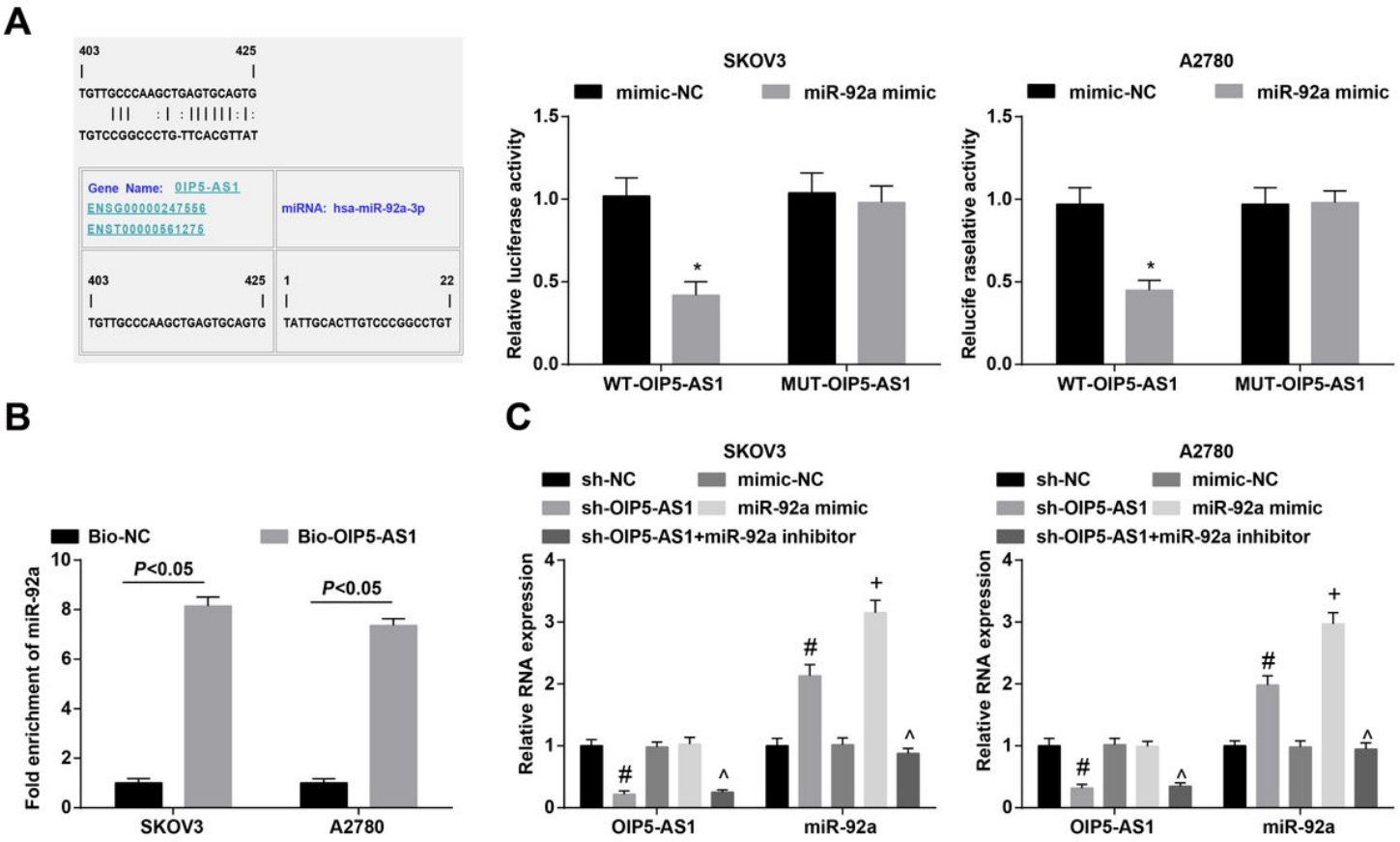

Figure 5

MiR-92a is a target of OIP5-AS1. A, binding sites of miR-92a and OIP5-AS1 were predicted by a bioinformatic website and the relationship between miR-92a and OIP5-AS1 was confirmed by dual luciferase report gene assay; B, RNA pull-down assay was used to affirm the regulatory relation between miR-92a and OIP5-AS1; C, expression of OIP5-AS1 and miR-92a in OC cells was determined by RT-qPCR; * P < 0.05 vs the anti-NC group, + P < 0.05 vs the mimic-NC group, # P < 0.05 vs the sh-NC group, ^ P < 0.05 vs the sh-OIP5-AS1 group; N = 3, the measurement data conforming to the normal distribution were expressed as mean ± standard deviation, unpaired t-test was performed for comparisons between two groups, one-way ANOVA was used for comparisons among multiple groups and Tukey's post hoc test was used for pairwise comparisons after one-way ANOVA.

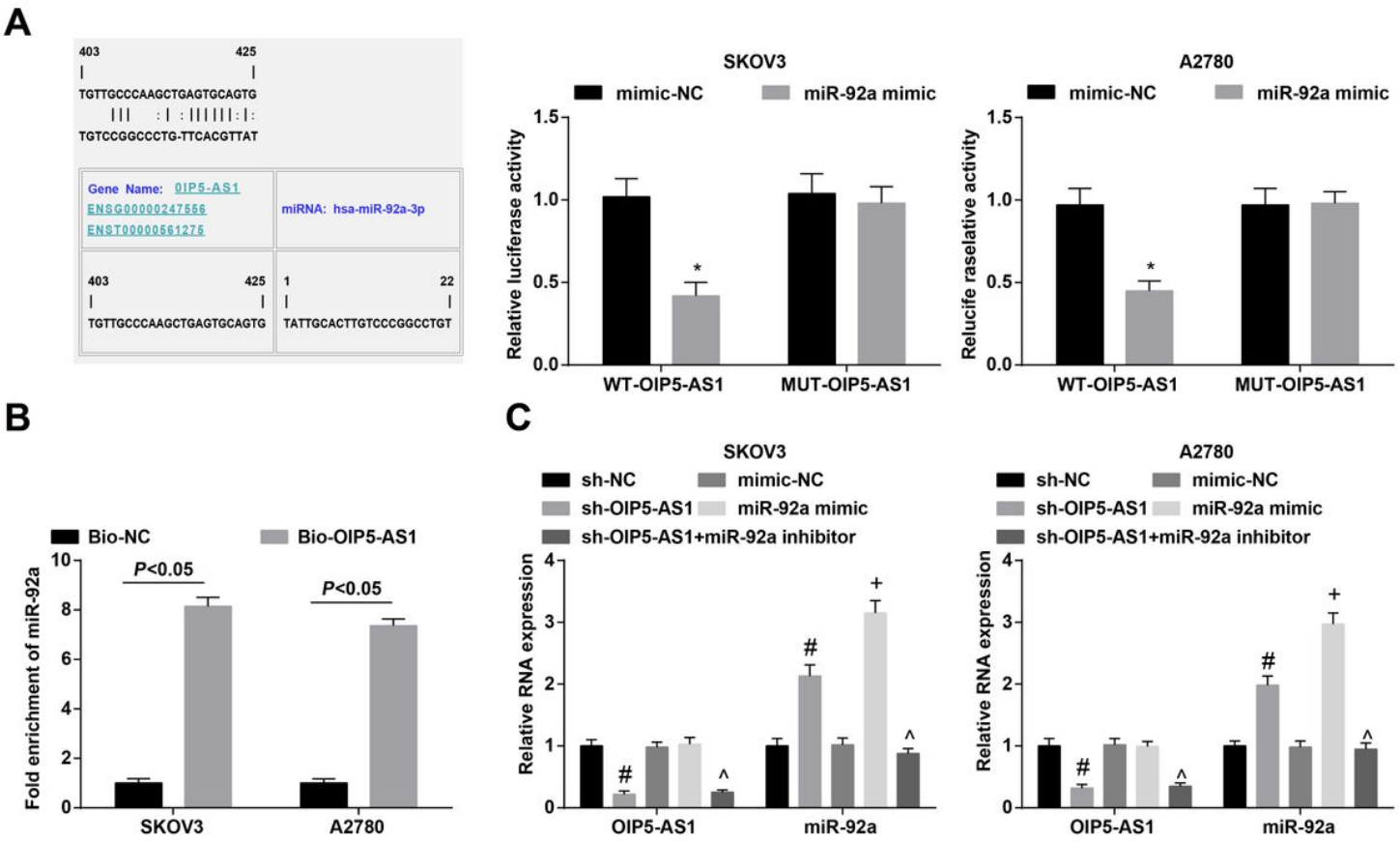

Figure 5

MiR-92a is a target of OIP5-AS1. A, binding sites of miR-92a and OIP5-AS1 were predicted by a bioinformatic website and the relationship between miR-92a and OIP5-AS1 was confirmed by dual luciferase report gene assay; B, RNA pull-down assay was used to affirm the regulatory relation between miR-92a and OIP5-AS1; C, expression of OIP5-AS1 and miR-92a in OC cells was determined by RT-qPCR; * P < 0.05 vs the anti-NC group, + P < 0.05 vs the mimic-NC group, # P < 0.05 vs the sh-NC group, ^ P < 0.05 vs the sh-OIP5-AS1 group; N = 3, the measurement data conforming to the normal distribution were expressed as mean ± standard deviation, unpaired t-test was performed for comparisons between two groups, one-way ANOVA was used for comparisons among multiple groups and Tukey's post hoc test was used for pairwise comparisons after one-way ANOVA.

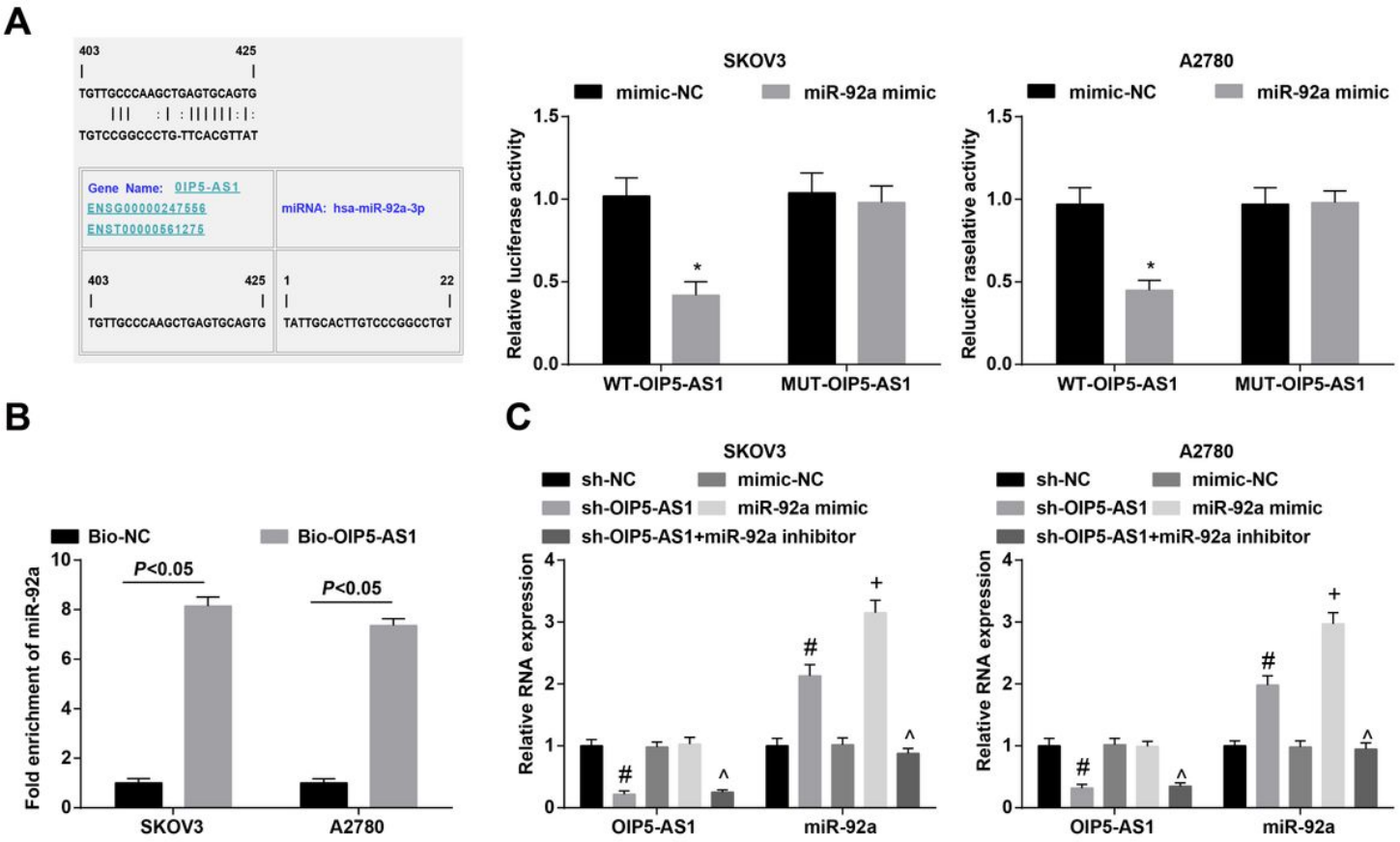

Figure 5

MiR-92a is a target of OIP5-AS1. A, binding sites of miR-92a and OIP5-AS1 were predicted by a bioinformatic website and the relationship between miR-92a and OIP5-AS1 was confirmed by dual luciferase report gene assay; B, RNA pull-down assay was used to affirm the regulatory relation between miR-92a and OIP5-AS1; C, expression of OIP5-AS1 and miR-92a in OC cells was determined by RT-qPCR; * P < 0.05 vs the anti-NC group, + P < 0.05 vs the mimic-NC group, # P < 0.05 vs the sh-NC group, ^ P < 0.05 vs the sh-OIP5-AS1 group; N = 3, the measurement data conforming to the normal distribution were expressed as mean ± standard deviation, unpaired t-test was performed for comparisons between two groups, one-way ANOVA was used for comparisons among multiple groups and Tukey's post hoc test was used for pairwise comparisons after one-way ANOVA.

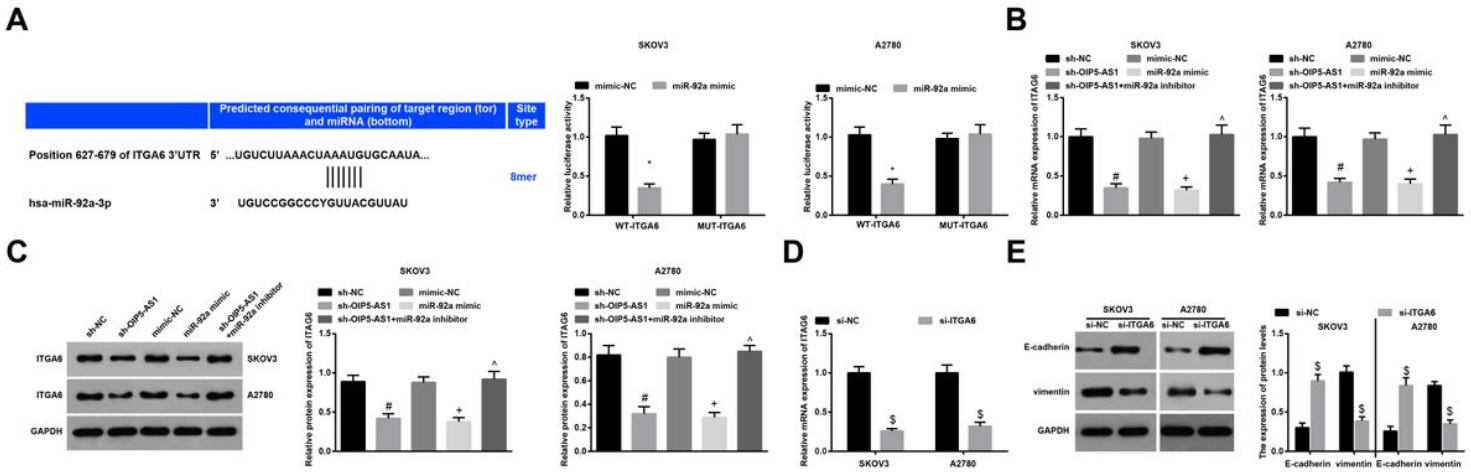

Figure 6

ITGA6 is targeted by miR-92a and the reduction of ITGA6 inhibits EMT of OC cells. A, binding sites of miR-92a and ITGA6 were predicted by a bioinformatic website and the relationship between miR-92a and ITGA6 was confirmed by dual luciferase report gene assay; B, ITGA6 expression in OC cells was assessed by RT-qPCR; C, protein expression of ITGA6 in OC cells was detected by Western blot analysis; D, ITGA6 mRNA expression in OC cells was detected by RT-qPCR; E, expression of EMT-related proteins was determined by Western blot analysis; * $P < 0.05$ vs the anti-NC group, + $P < 0.05$ vs the mimic-NC group, # $P < 0.05$ vs the sh-NC group, ^ $P < 0.05$ vs the sh-OIP5-AS1 group, $ $P < 0.05$ vs the si-NC group; N = 3, the measurement data conforming to the normal distribution were expressed as mean ± standard deviation, unpaired t-test was performed for comparisons between two groups, one-way ANOVA was used for comparisons among multiple groups and Tukey's post hoc test was used for pairwise comparisons after one-way ANOVA.

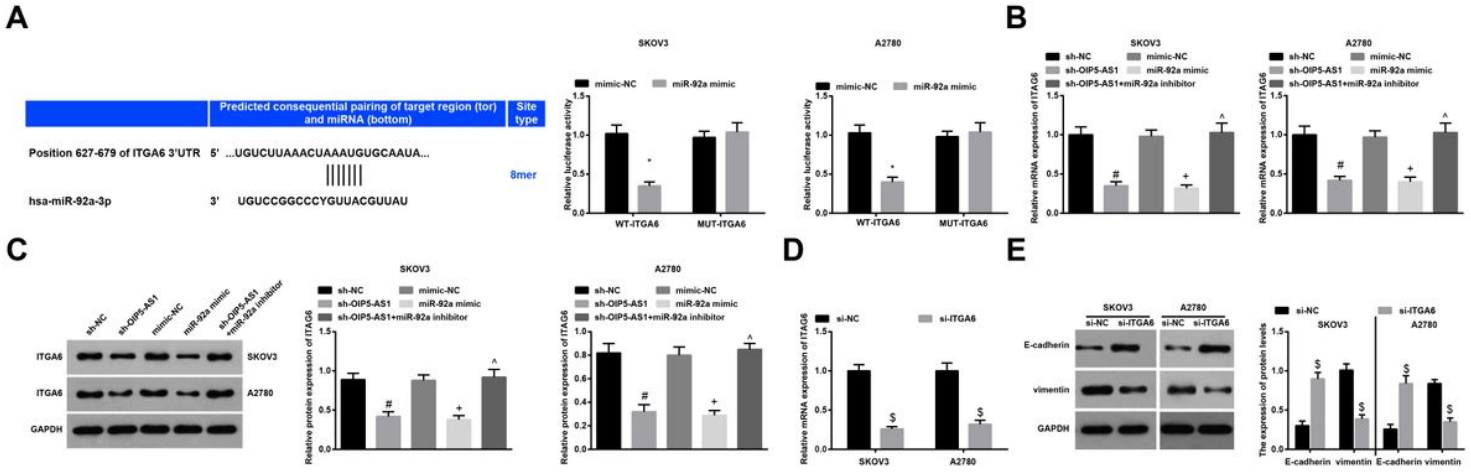

Figure 6

ITGA6 is targeted by miR-92a and the reduction of ITGA6 inhibits EMT of OC cells. A, binding sites of miR-92a and ITGA6 were predicted by a bioinformatic website and the relationship between miR-92a and ITGA6 was confirmed by dual luciferase report gene assay; B, ITGA6 expression in OC cells was assessed

by RT-qPCR; C, protein expression of ITGA6 in OC cells was detected by Western blot analysis; D, ITGA6 mRNA expression in OC cells was detected by RT-qPCR; E, expression of EMT-related proteins was determined by Western blot analysis; * P < 0.05 vs the anti-NC group, + P < 0.05 vs the mimic-NC group, # P < 0.05 vs the sh-NC group, ^ P < 0.05 vs the sh-OIP5-AS1 group, $ P < 0.05 vs the si-NC group; N = 3, the measurement data conforming to the normal distribution were expressed as mean ± standard deviation, unpaired t-test was performed for comparisons between two groups, one-way ANOVA was used for comparisons among multiple groups and Tukey's post hoc test was used for pairwise comparisons after one-way ANOVA.

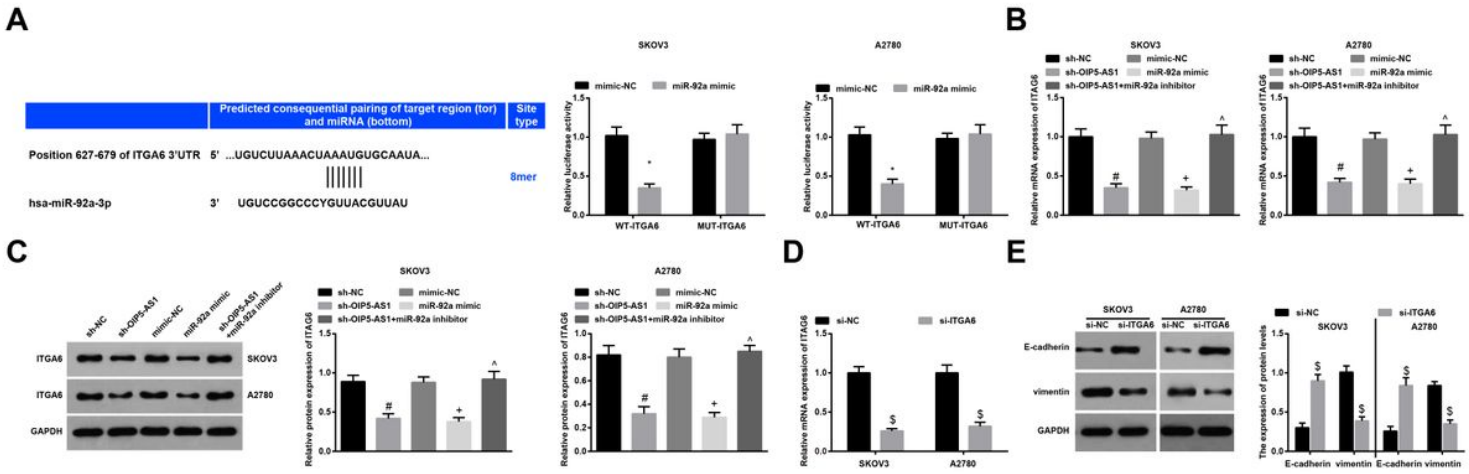

Figure 6

ITGA6 is targeted by miR-92a and the reduction of ITGA6 inhibits EMT of OC cells. A, binding sites of miR-92a and ITGA6 were predicted by a bioinformatic website and the relationship between miR-92a and ITGA6 was confirmed by dual luciferase report gene assay; B, ITGA6 expression in OC cells was assessed by RT-qPCR; C, protein expression of ITGA6 in OC cells was detected by Western blot analysis; D, ITGA6 mRNA expression in OC cells was detected by RT-qPCR; E, expression of EMT-related proteins was determined by Western blot analysis; * P < 0.05 vs the anti-NC group, + P < 0.05 vs the mimic-NC group, # P < 0.05 vs the sh-NC group, ^ P < 0.05 vs the sh-OIP5-AS1 group, $ P < 0.05 vs the si-NC group; N = 3, the measurement data conforming to the normal distribution were expressed as mean ± standard deviation, unpaired t-test was performed for comparisons between two groups, one-way ANOVA was used for comparisons among multiple groups and Tukey's post hoc test was used for pairwise comparisons after one-way ANOVA.

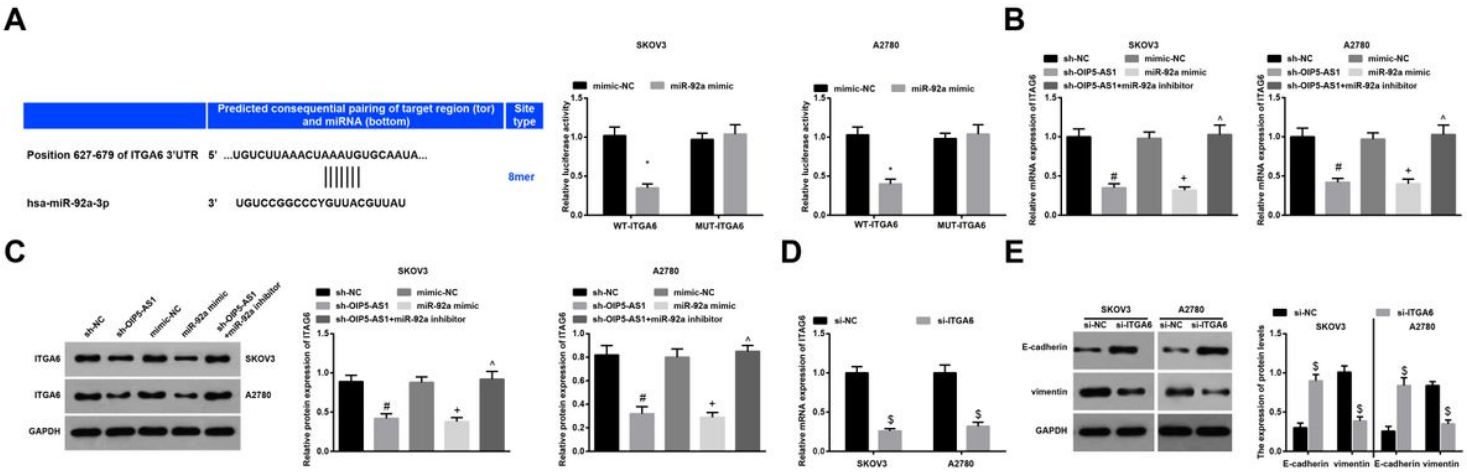

Figure 6

ITGA6 is targeted by miR-92a and the reduction of ITGA6 inhibits EMT of OC cells. A, binding sites of miR-92a and ITGA6 were predicted by a bioinformatic website and the relationship between miR-92a and ITGA6 was confirmed by dual luciferase report gene assay; B, ITGA6 expression in OC cells was assessed by RT-qPCR; C, protein expression of ITGA6 in OC cells was detected by Western blot analysis; D, ITGA6 mRNA expression in OC cells was detected by RT-qPCR; E, expression of EMT-related proteins was determined by Western blot analysis; * $P < 0.05$ vs the anti-NC group, + $P < 0.05$ vs the mimic-NC group, # $P < 0.05$ vs the sh-NC group, ^ $P < 0.05$ vs the sh-OIP5-AS1 group, $ $P < 0.05$ vs the si-NC group; N = 3, the measurement data conforming to the normal distribution were expressed as mean ± standard deviation, unpaired t-test was performed for comparisons between two groups, one-way ANOVA was used for comparisons among multiple groups and Tukey's post hoc test was used for pairwise comparisons after one-way ANOVA.